UNIVERSITÀ DELLA CALABRIA
DIMES
April 9 – 11, 2019

Introduction to Microwave Imaging Part III: Performance Metrics, Filtering, Tissue Imaging

Natalia K. Nikolova
nikolova@ieee.org

McMaster University
Department of Electrical and Computer Engineering
Electromagnetic Vision (EMVi) Research Laboratory
Hamilton, ON CANADA

COURSE OVERVIEW

Day 1: Introduction & Forward Models of Microwave Imaging
- Field-based Integral Solutions of the Scattering Problem in Time and Frequency
- Born and Rytov Approximations of the Forward Model of Scattering
- Scattering Parameters and Integral Solutions in terms of *S*-parameters
- 2D Model of Tomography in Microwave Scattering

Day 2: Linear Inversion Methods
- Deconvolution Methods
  - Microwave Holography (MH)
  - Scattered Power Mapping (SPM)
- Image Reconstruction of Pulsed-radar Data
  - Synthetic Focusing: Delay and Sum (DAS)

Day 3: Performance Metrics & Hardware
- Spatial Resolution
- Dynamic Range
- Data Signal-to-noise Ratio

Select Topics
- Overview of Nonlinear Inversion Methods
  - Direct Iterative Methods
  - Model-based Optimization Methods
- Tissue Imaging – Challenges and Advancements

PERFORMANCE METRICS:
SPATIAL RESOLUTION

[Nikolova, *Introduction to Microwave Imaging*, 2017]

- **definition of spatial resolution limit**: the smallest shape detail of an imaged object correctly represented in its image
- spatial resolution in a general direction $\hat{\mathbf{s}}$ (derivation based on far-zone scattering)

$v_b/(2B)$ with scanning

$$\delta r'(\hat{\mathbf{s}}) = \boxed{\frac{v_b}{B}} \cdot \frac{1}{|\cos\theta_1 + \cos\theta_2|}$$

signal frequency bandwidth

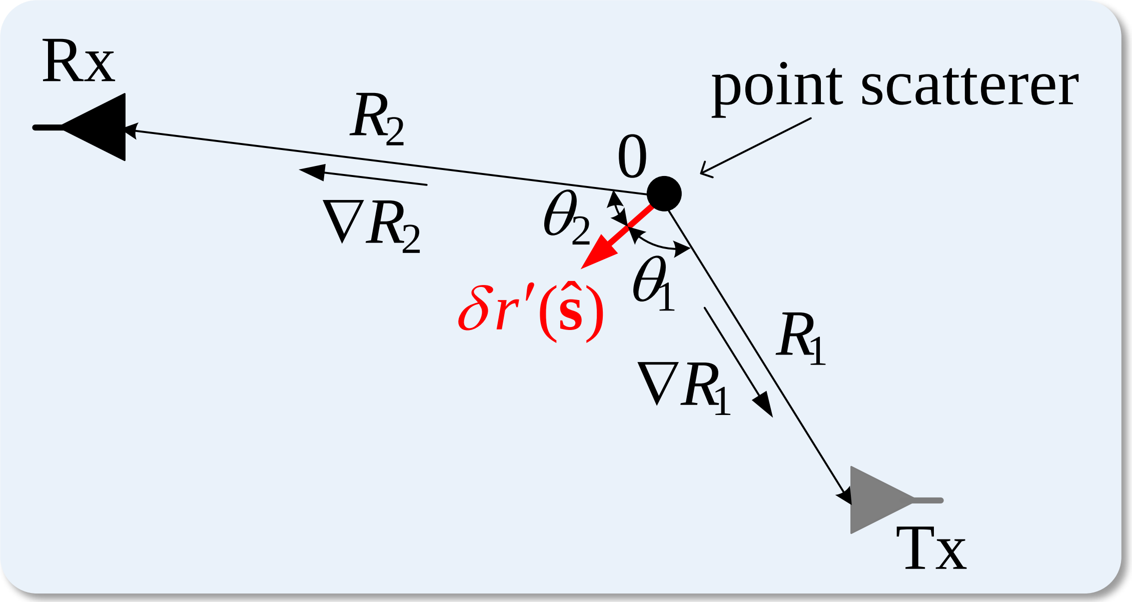

- resolution depends strongly on the position of the Tx&Rx antennas relative to the imaged voxel
- best case: $\theta_1 = \theta_2 = 0$ or $\theta_1 = \theta_2 = \pi$

SPATIAL RESOLUTION LIMITS: SCENARIOS

$$\delta r'(\hat{\mathbf{s}}) = \frac{v_b}{B} \cdot \frac{1}{|\cos\theta_1 + \cos\theta_2|}$$

- <u>best case</u>: $\theta_1 = \theta_2 = 0$ or $\theta_1 = \theta_2 = \pi$

  example - monostatic radar (reflection or back-scatter measurements) has best resolution along range axis (*aka* ***range*** or ***depth*** resolution)

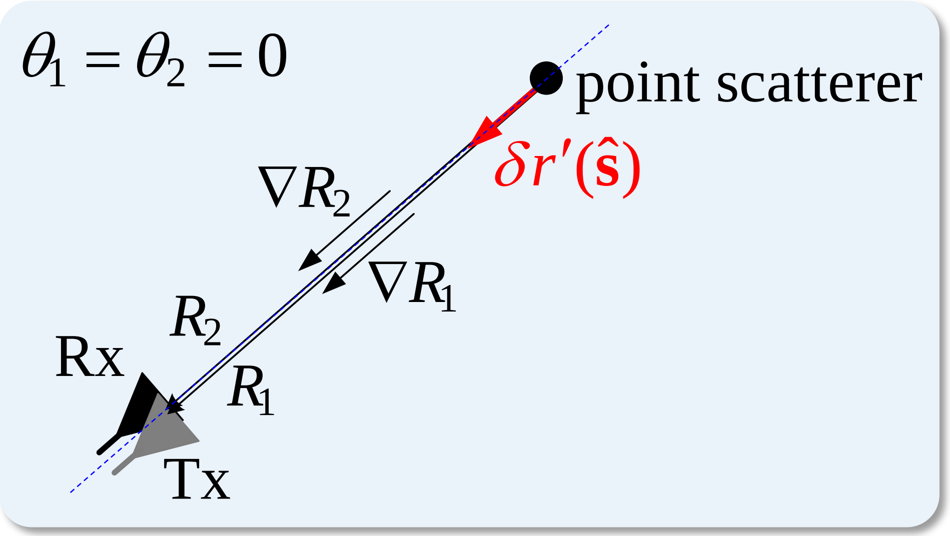

- <u>worst case #1</u>: $\theta_1, \theta_2 = \pm 90°$

  $\delta r' \to \infty$ (complete loss of resolution)

  example - monostatic radar has no ***cross-range*** (***lateral***) resolution without scanning

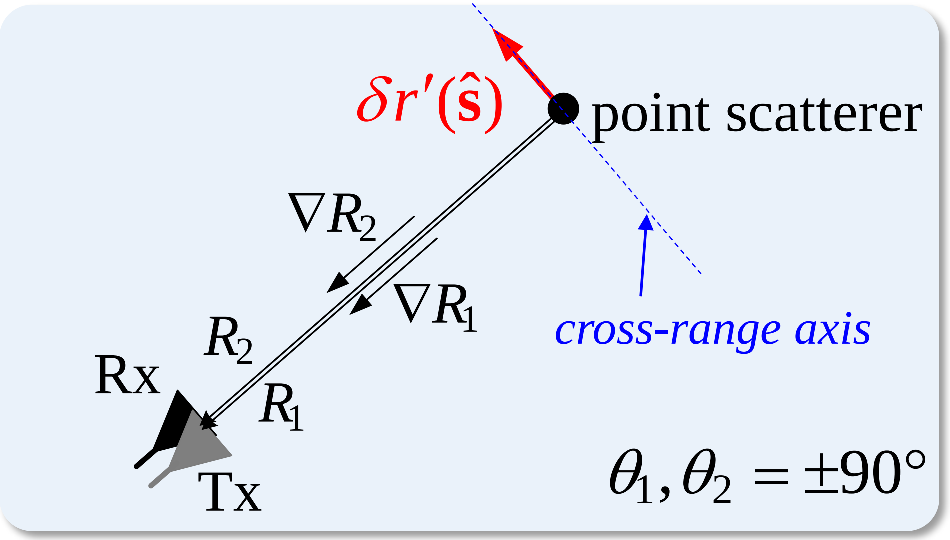

SPATIAL RESOLUTION LIMITS: SCENARIOS – 2

- worst case #2: $\theta_2 = \pi - \theta_1$

example – bi-static radar with Tx & Rx antennas aligned along boresight has no resolution along both range and cross-range axes if target is on the boresight line

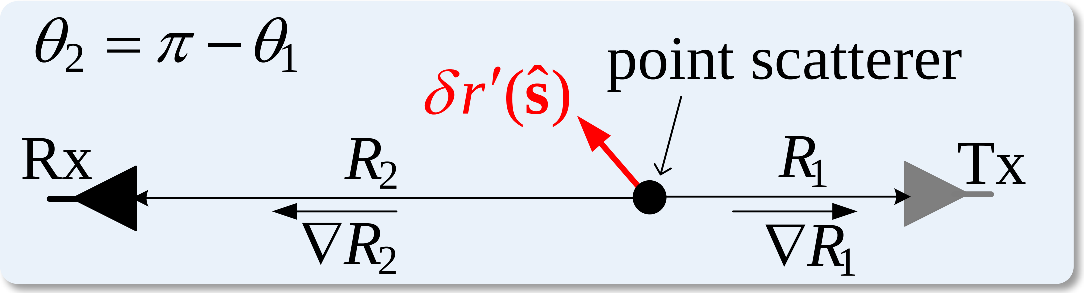

- implications
  - ➢ imaging is impossible with a single static Tx/Rx antenna bore-sight aligned pair
  - ➢ mechanical or electronic scanning of Tx or Rx or both antennas is required to achieve a variety of viewing angles θ_1 and θ_2
  - ➢ best viewing angles provided by scanning on closed surfaces (spherical, cylindrical) around target – rarely possible in practice
  - ➢ wide-beam antennas are preferred

FUNDAMENTAL SPATIAL RESOLUTION LIMITS

- fundamental resolution limit is the best possible range or cross-range limit

$$\delta_r = \frac{v_\mathrm{b}}{2B} \text{ or } \delta_r = \frac{v_\mathrm{b}}{2 f_{\max}} = \frac{\lambda_\mathrm{b}^{\min}}{2}$$

- for isotropic antennas and full-range of viewing angles from $-\pi$ to $+\pi$, effective bandwidth is doubled **[Nikolova, *Introduction to Microwave Imaging*, 2017]**

$$\delta r'(\hat{\mathbf{s}}) = \frac{v_\mathrm{b}}{2B} \cdot \frac{1}{|\cos\theta_1 + \cos\theta_2|} \Rightarrow \delta_r = \frac{v_\mathrm{b}}{4B} \text{ or } \delta_r = \frac{\lambda_\mathrm{b}^{\min}}{4}$$

- ***only near-zone imaging can overcome the fundamental resolution limit*** IF the fast-varying spatial distribution of the near-field scattering can be measured (its strength must exceeds system noise)

PERFORMANCE METRICS:
DATA CONSTRAST-TO-NOISE RATIO (CNR)

[results presented at EuCAP’19, courtesy of Daniel Tajik, Ph.D. student]

DATA QUALITY

- the quality of the measured responses is critical for the image fidelity
- major factors degrading data quality
  - radar clutter: reflections from components of the imaging setup
  - positioning errors
  - electronic noise
- metrics for data quality: SNR, CNR
- consequences of poor data quality
  - reduced system sensitivity
  - … which leads to loss of resolution
- **objectives of data-quality control**: (i) identify and remove low-quality data, (ii) provide metric for an overall system performance

DATA QUALITY ESTIMATION USING MEASURED PSFs

- typical PSF data in a tissue-imaging experiment with transmission *S*-parameters

<u>Reference Object</u>

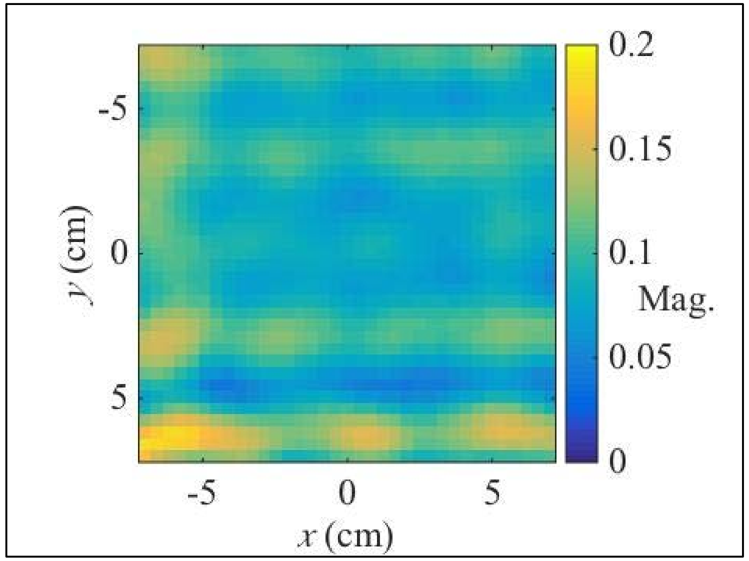

<u>Calibration Object</u>

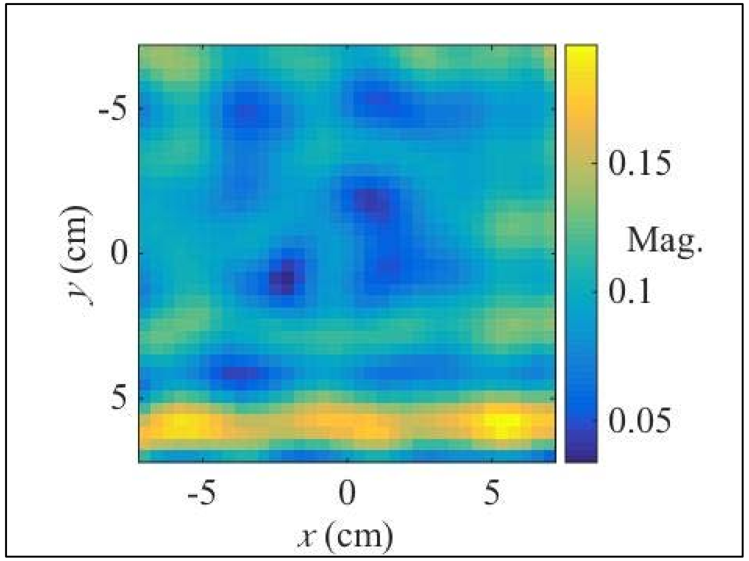

<u>Point Spread Function</u>

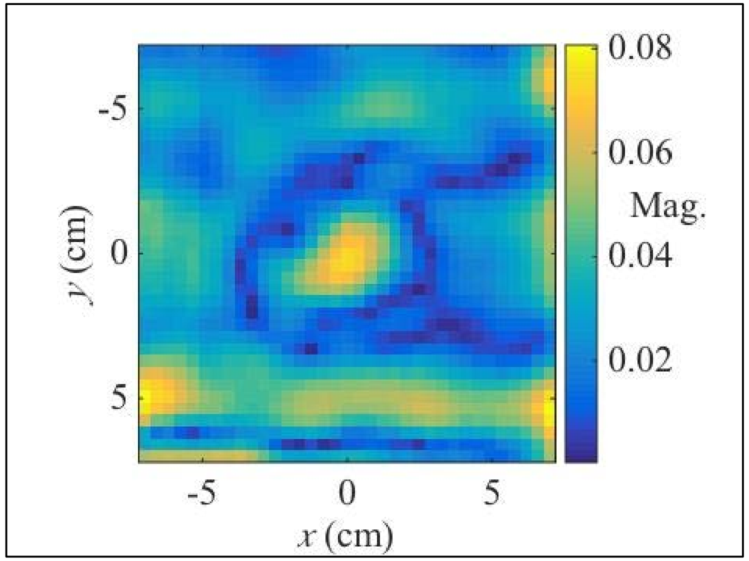

$$(S_{ik}^{\mathrm{sc}})_{\mathrm{B}} = S_{ik}^{\mathrm{OUT}} - S_{ik}^{\mathrm{RO}}$$

- incomplete background clutter removal due to positioning uncertainties

DATA QUALITY ESTIMATION USING CNR METRIC

region separation

- signal region A_s
- exclusion zone A_e
- background A_b

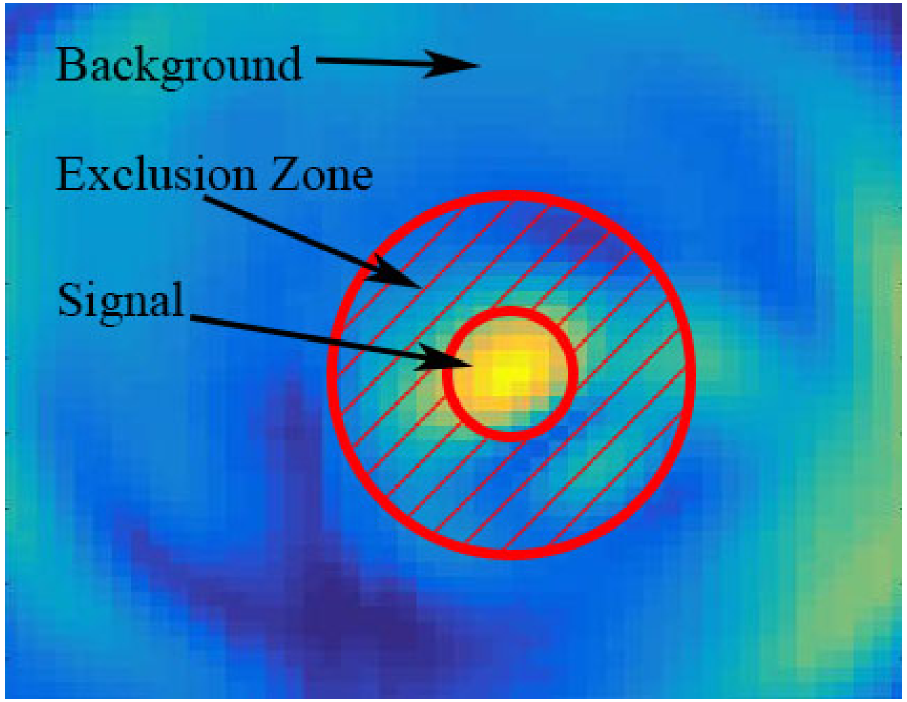

Image Credit: Daniel Tajik

CNR threshold

- depends on reconstruction algorithm – 3-dB is typical

data contrast-to-noise ratio calculation

$$\mathrm{CNR}(\omega)=\frac{\mathrm{average}\left(S_{ik}^{\mathrm{PSF}}\left(A_\mathrm{s},\omega\right)\right)-\mathrm{average}\left(S_{ik}^{\mathrm{PSF}}\left(A_\mathrm{b},\omega\right)\right)}{\mathrm{std}\left(S_{ik}^{\mathrm{PSF}}\left(A_\mathrm{b},\omega\right)\right)}$$

$$\mathrm{average}(D)=|\bar{d}|=\left|\frac{1}{N}\sum_{i=1}^{N}d_i\right|$$

$$\mathrm{std}(D)=\left(\frac{1}{N-1}\sum_{i=1}^{N}|d_i-\bar{d}|^2\right)^{1/2}$$

CNR EXAMPLE: PLANAR SCANNING FOR BREAST-PHANTOM EXPERIMENTS

- Tx: TEM horn, Rx: 9 element bowtie array
- platform raster scans along *x*, *y*
- tray holds embedding medium, OUT, CO and RO
- frequency range from 3 GHz to 8 GHz (100 MHz steps)

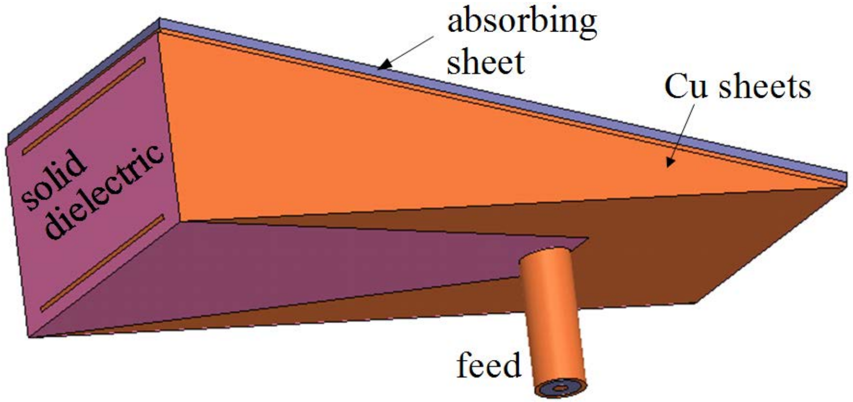

[Amineh *et al.*, *IEEE Trans. Antennas Propag.*, 2011]

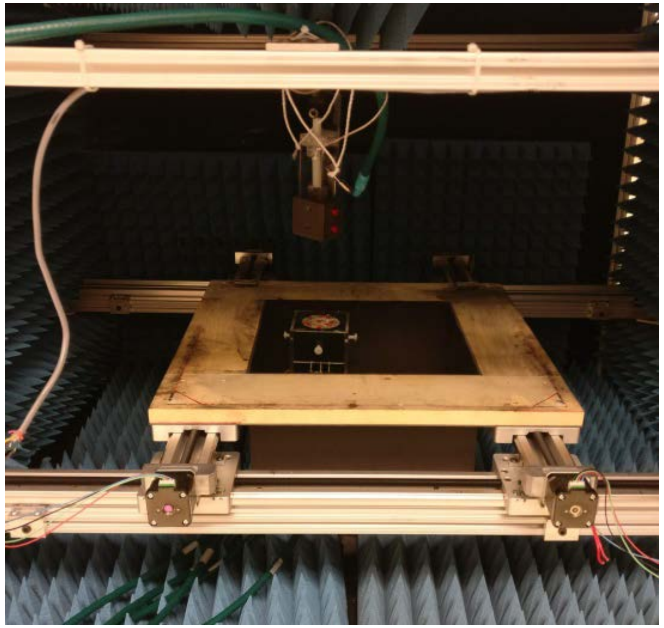

Image Credit: Daniel Tajik

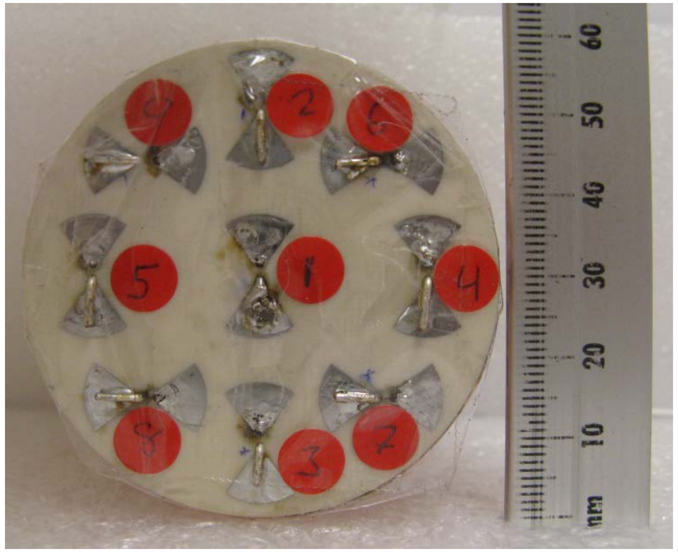

[Photo credit: Justin J. McCombe]
[Amineh *et al.*, *IEEE Trans. Instr. Meas.*, 2015]

CNR EXAMPLE: SETUP IN ACQUIRING THE PSF

- desired resolution ≈ **1 cm^3**
- approximate tumour relative permittivity ≈ **50 – i25**
- **Reference Object (RO):** averaged Type-2 breast tissue ($\boldsymbol{\varepsilon_{r,b}}$ **≈ 10 – i5**)

  Type 2: 25%-50% fibroglandular tissue, remaing adipose (fatty) tissue
- **Calibration Object (CO):** same embedding medium, with central scattering probe
- scattering probe (cylinder): diameter = **1 cm**, height = **1 cm**
- scattering probe permittivity ≈ cancerous tissue, $\boldsymbol{\varepsilon_{r,sp}}$ **= 50 – i0.5**

CNR EXAMPLE: RESULTS

- over 50% frequencies above 3 dB CNR
  - ➢ system deemed of acceptable quality to proceed with OUT imaging
  - ➢ system expected to have sufficient resolution (1 cm^3)
- several poor frequencies, possibly due to antenna impedance mismatch – to be removed from data set

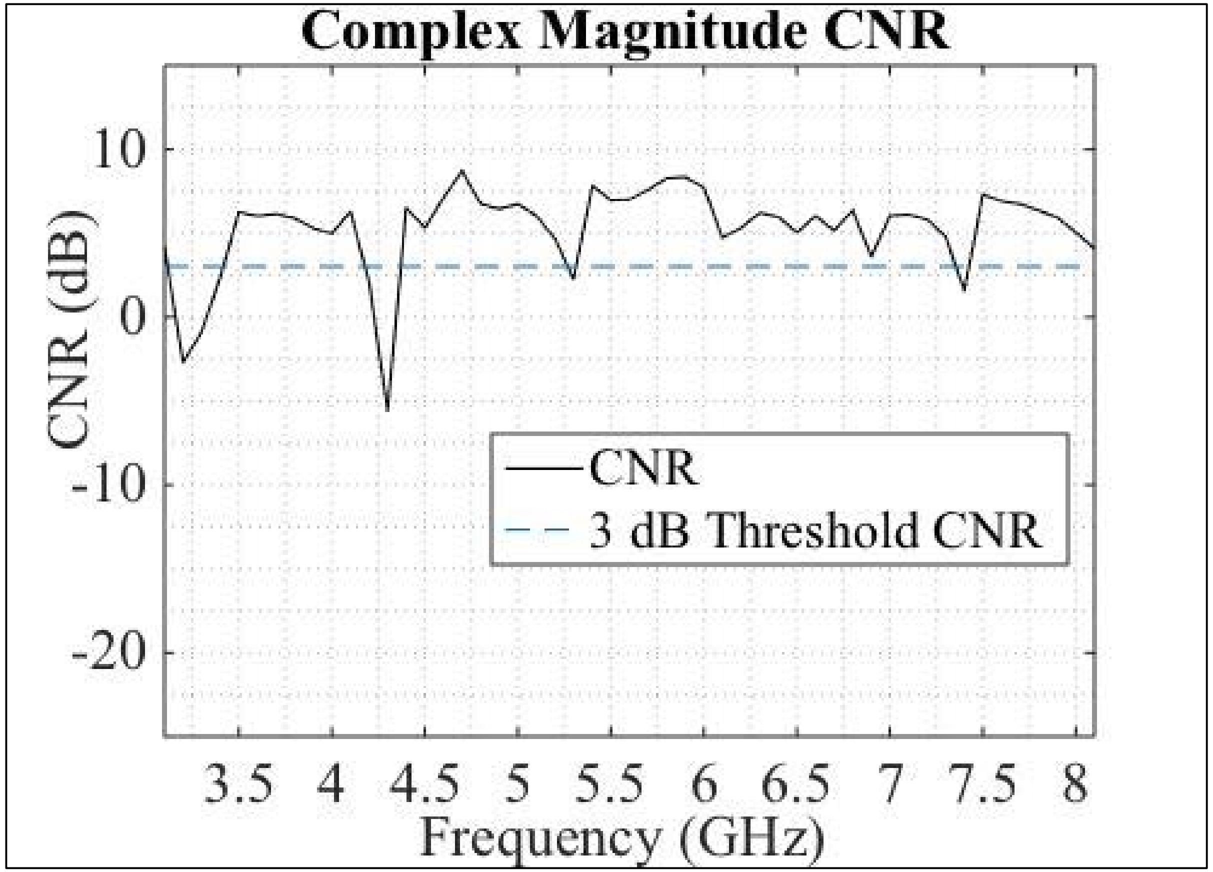

CNR EXAMPLE: TISSUE PHANTOMS

- phantom: five 1.1 cm thick carbon rubber sheets stacked
- filled with fibroglandular&tumour simulants
- simulants surrounded with matched medium

Tissue	Color	Permittivity (5 GHz)
Tumour Simulant	**Blue Circles**	50 — 25i
Fibroglandular Simulant	**White**	13 — 6i
Averaged Type-2 Breast Tissue	**Brown**	7 — 3i
Absorbing Foam	**Black**	10 — 3i

layer 2

layer 4

CNR EXAMPLE: IMPACT OF DATA “CLEAN UP” (BORN HOLOGRAPHY)

- CNR filtering sharpens image & reduces weaker ringing artifacts

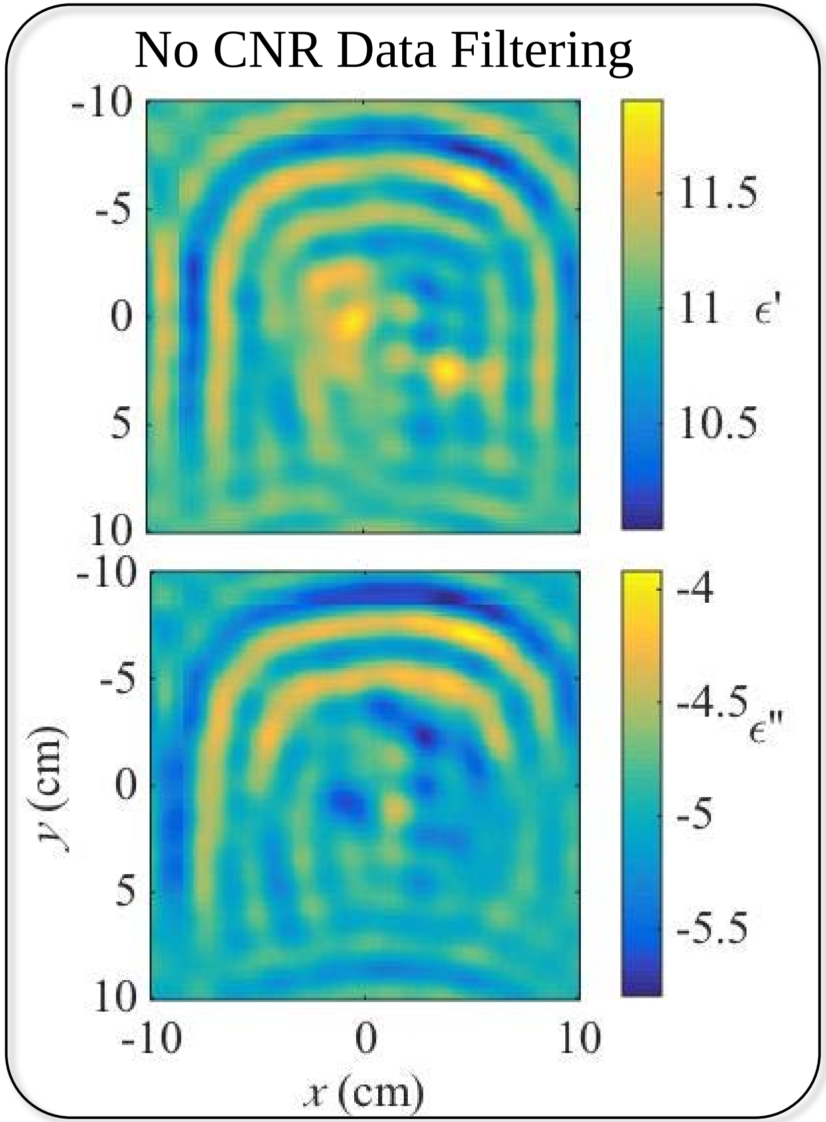

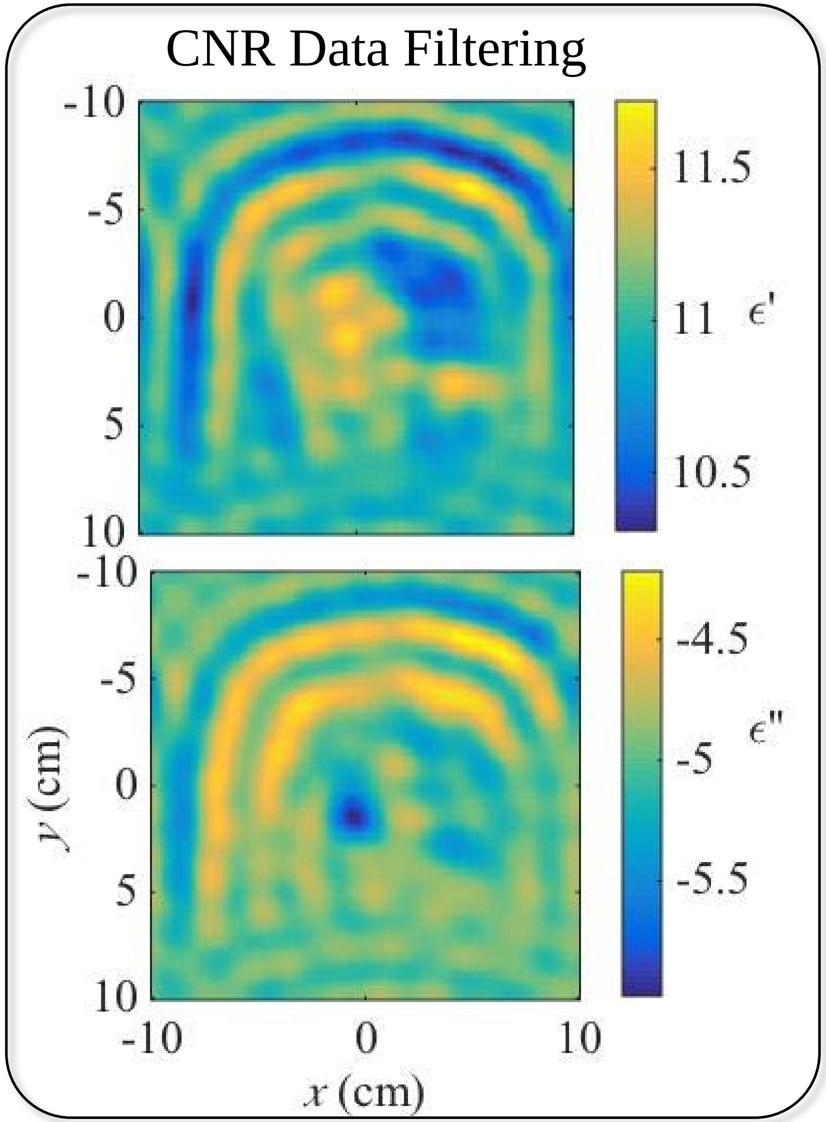

layer 2

layer 4

FILTERING STRATEGIES FOR INVERSION IN FOURIER SPACE: APODIZATION AND FILTERING IN FOURIER SPACE

[results courtesy of Daniel Tajik, Ph.D. student]

APODIZATION: DATA FILTERING IN REAL (X-Y) SPACE

- apodization (edge) filtering is used to reduce "ringing" artifacts generated by FFT of data
- widely used in photography, ultrasound and MR imaging
- apodization is a mandatory step when inversion is done in Fourier (or *k*) space, especially when signal strength is significant at the edge of the acquisition aperture
- let us re-visit a simulation experiment with microwave holography

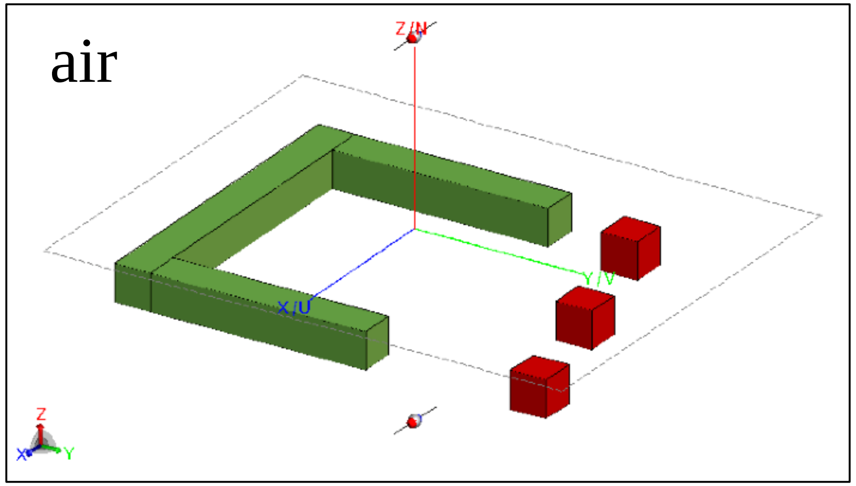

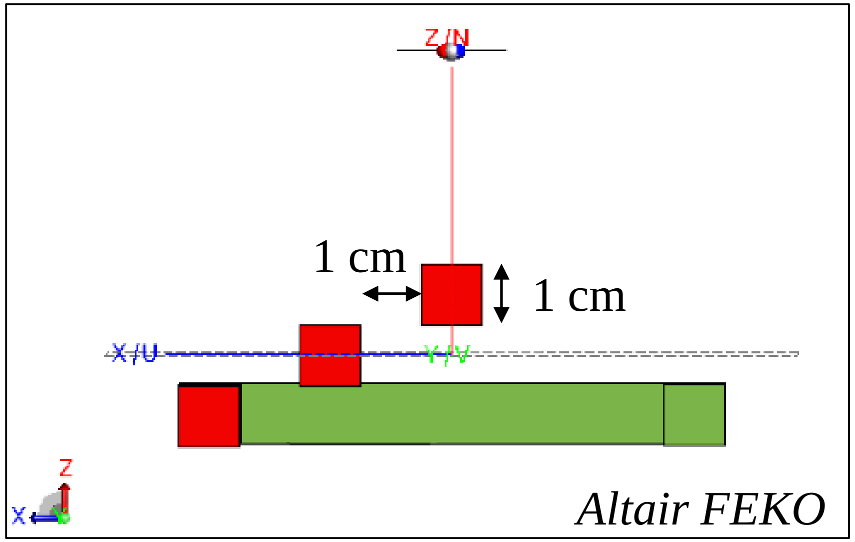

[Tajik *et al.*, *JPIER*-B 2017]

THE NEED FOR APODIZATION: EXAMPLE

[Tajik *et al.*, *JPIER*-B 2017]

- edge "discontinuities" lead to Gibb's artifacts ("ringing") in Fourier space
- this corrupts the reconstruction leading to noise-like images in real space

artificially added edge artifact

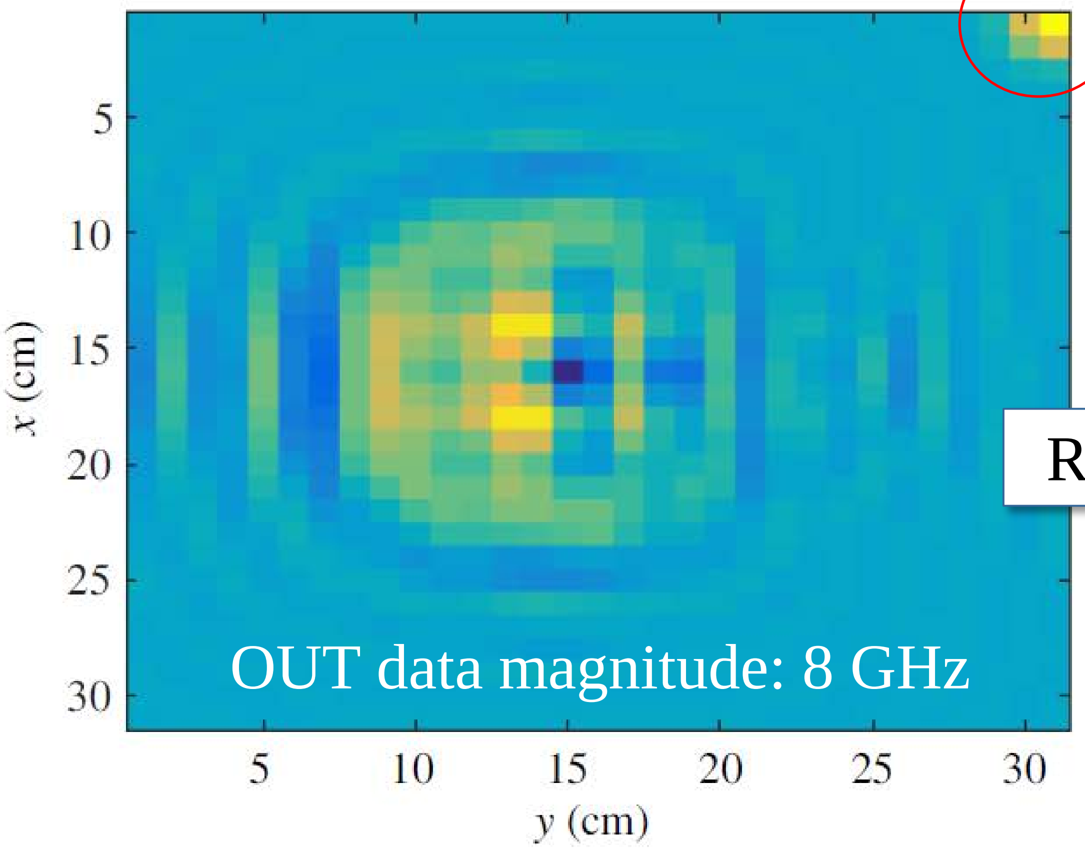

Rytov QMH

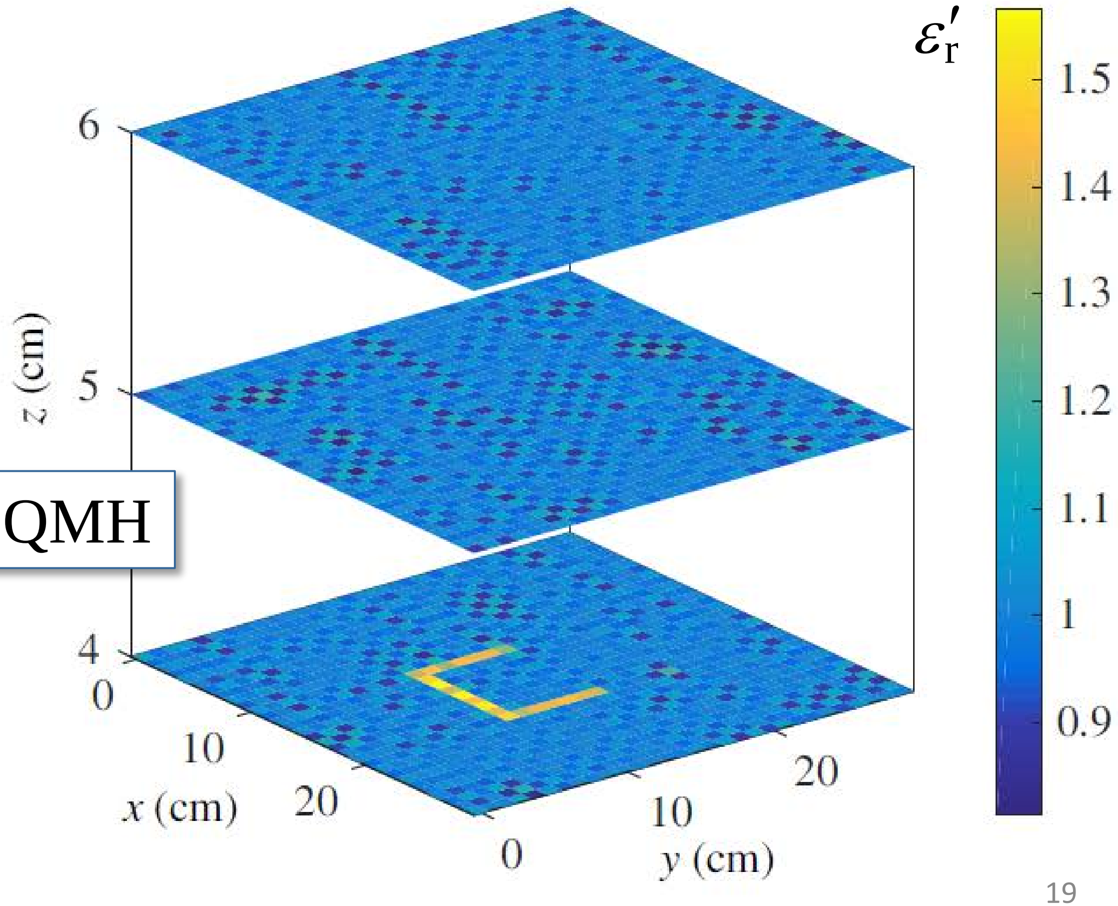

APODIZATION FILTERING: EXAMPLE

[Tajik *et al.*, *JPIER*-B 2017]

- apodization filtering aims at tapering down to zero the signal strength at the aperture edges

<u>2-D cosine apodization filter</u>

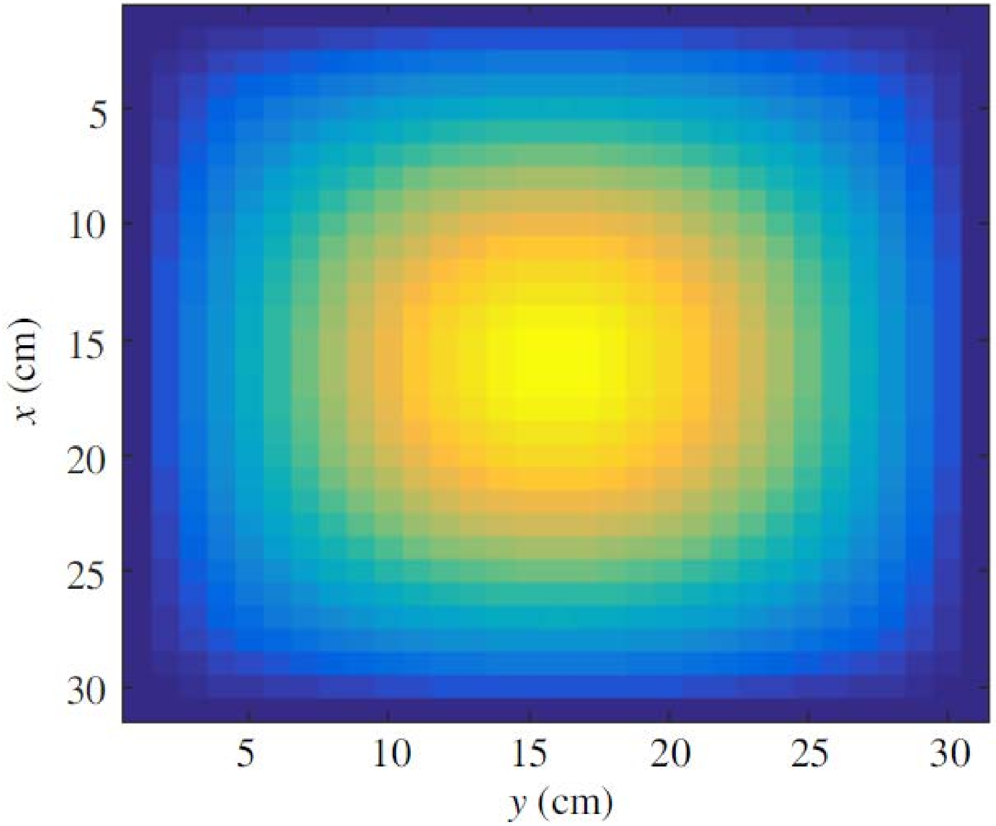

<u>image reconstructed with data filtered by the 2-D cosine function</u>

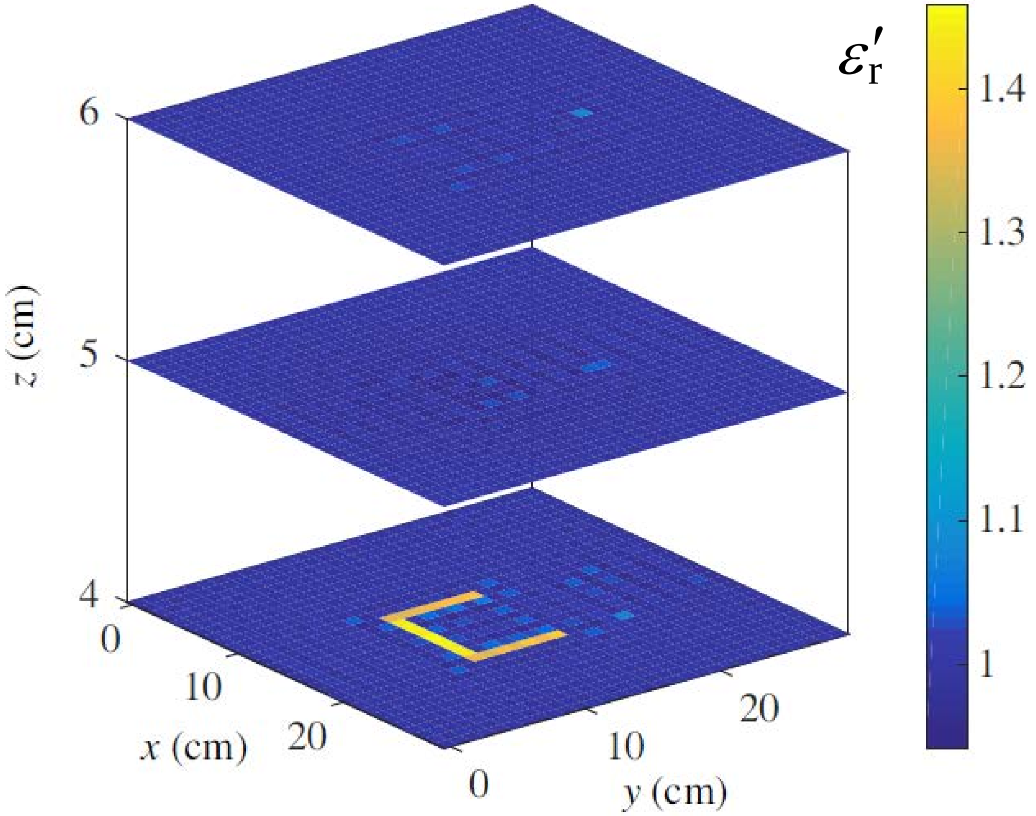

POST-INVERSION FILTERING IN FOURIER SPACE

- inversion in k-space involves solving systems of equations one $\boldsymbol{\kappa} = (k_x, k_y)$ point at a time

<u>microwave holography</u>

$$\begin{bmatrix} \left[\tilde{S}_0^{\mathrm{PSF}}(\boldsymbol{\kappa}_{ij}; z_1')\right]^{(1)} & \cdots & \left[\tilde{S}_0^{\mathrm{PSF}}(\boldsymbol{\kappa}_{ij}; z_{N_z}')\right]^{(1)} \\ \vdots & \ddots & \vdots \\ \left[\tilde{S}_0^{\mathrm{PSF}}(\boldsymbol{\kappa}_{ij}; z_1')\right]^{(N_\omega)} & \cdots & \left[\tilde{S}_0^{\mathrm{PSF}}(\boldsymbol{\kappa}_{ij}; z_{N_z}')\right]^{(N_\omega)} \end{bmatrix}_{N_\omega N_T \times N_z} \cdot \begin{bmatrix} \tilde{f}(\boldsymbol{\kappa}_{ij}; z_1') \\ \vdots \\ \tilde{f}(\boldsymbol{\kappa}_{ij}; z_{N_z}') \end{bmatrix}_{N_z \times 1} = \begin{bmatrix} \tilde{S}^{(1)}(\boldsymbol{\kappa}_{ij}) \\ \vdots \\ \tilde{S}^{(N_\omega)}(\boldsymbol{\kappa}_{ij}) \end{bmatrix}_{N_\omega N_T \times 1}$$

<u>scattered-power mapping</u>

$$\begin{bmatrix} \tilde{M}_{\mathrm{sp}@(0,0,z_1)}(\boldsymbol{\kappa}_{ij}, z_1) & \cdots & \tilde{M}_{\mathrm{sp}@(0,0,z_{N_z})}(\boldsymbol{\kappa}_{ij}, z_1) \\ \vdots & \ddots & \vdots \\ \tilde{M}_{\mathrm{sp}@(0,0,z_1)}(\boldsymbol{\kappa}_{ij}, z_{N_z}) & \cdots & \tilde{M}_{\mathrm{sp}@(0,0,z_{N_z})}(\boldsymbol{\kappa}_{ij}, z_{N_z}) \end{bmatrix}_{N_z \times N_z} \cdot \begin{bmatrix} \tilde{f}(\boldsymbol{\kappa}_{ij}, z_1) \\ \vdots \\ \tilde{f}(\boldsymbol{\kappa}_{ij}, z_{N_z}) \end{bmatrix}_{N_z \times 1} = \begin{bmatrix} \tilde{M}(\boldsymbol{\kappa}, z_1) \\ \\ \tilde{M}(\boldsymbol{\kappa}, z_{N_z}) \end{bmatrix}_{N_z \times 1}$$

POST-INVERSION FILTERING IN FOURIER SPACE – 2

- oversampling – underlying reason for inversion errors
  - **advantage**: improves spatial resolution by capturing near-field scattering (fast variation along x and y → high spatial frequencies k_x and k_y)
  - **disadvantage**: if near-field scattering is weak (below noise), the results at high spatial frequencies k_x and k_y are erroneous → degrade the entire IFFT solution in (x,y)
- recommended sampling – based on plane-wave far-zone scattering (see Day 1 lecture)

$$\Delta\zeta \le \Delta\zeta_{max} \approx \frac{\lambda_b^{min}}{4\sin\alpha},\ \zeta \equiv x, y$$

typical choice

$$\Rightarrow \Delta\zeta = \frac{\lambda_b^{min}}{4}$$

$$\Rightarrow k_\zeta^{max} = \frac{\pi}{\Delta\zeta} = \boxed{\frac{4\pi}{\lambda_b^{min}}} \cdot \sin\alpha$$

chosen spatial-spectrum width

← *actual width*

viewing angle is limited

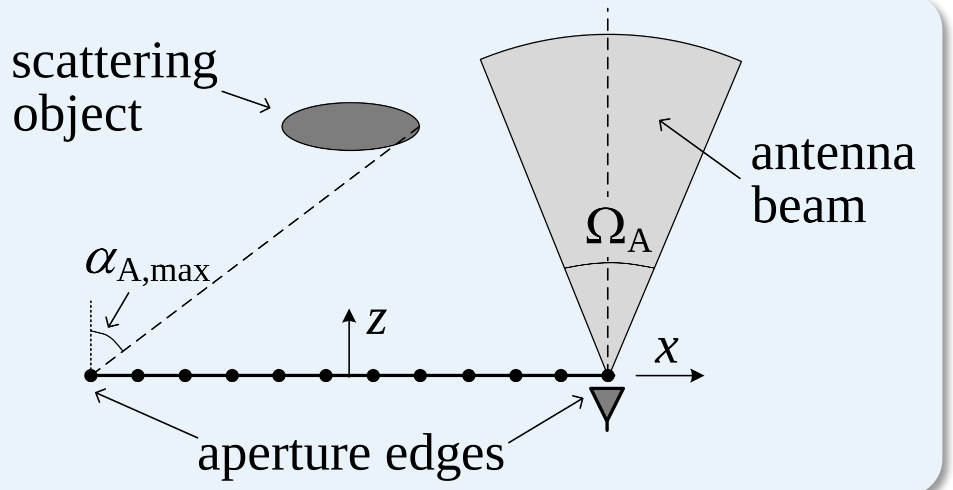

EXAMPLE: POST-INVERSION FILTERING

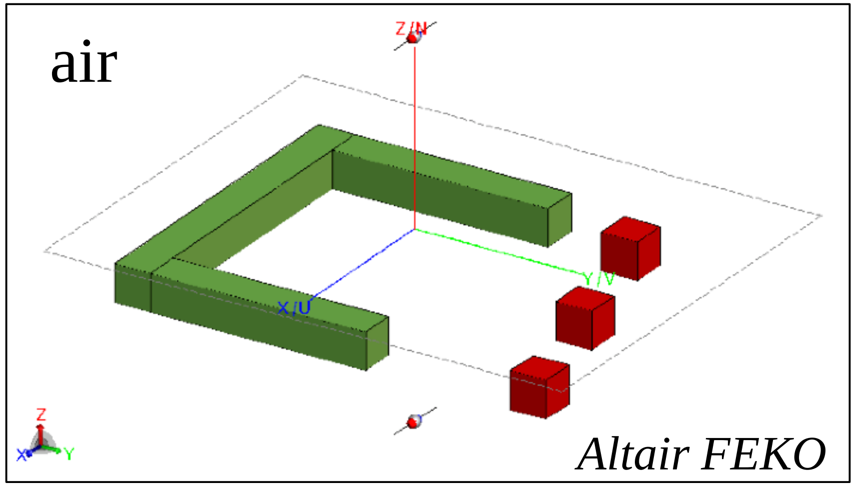

- data has no edge “discontinuities” here – apodization not needed
- maximum recommended sampling step
  $\Delta x_{\max} = \Delta y_{\max} \approx 1 \text{ cm} \rightarrow \bar{K}_{\max} = 100\pi \text{ rad/m}$
- sampling step chosen
  $\Delta x = \Delta y \approx 0.5 \text{ cm} \rightarrow K_{\max} = 200\pi \text{ rad/m}$

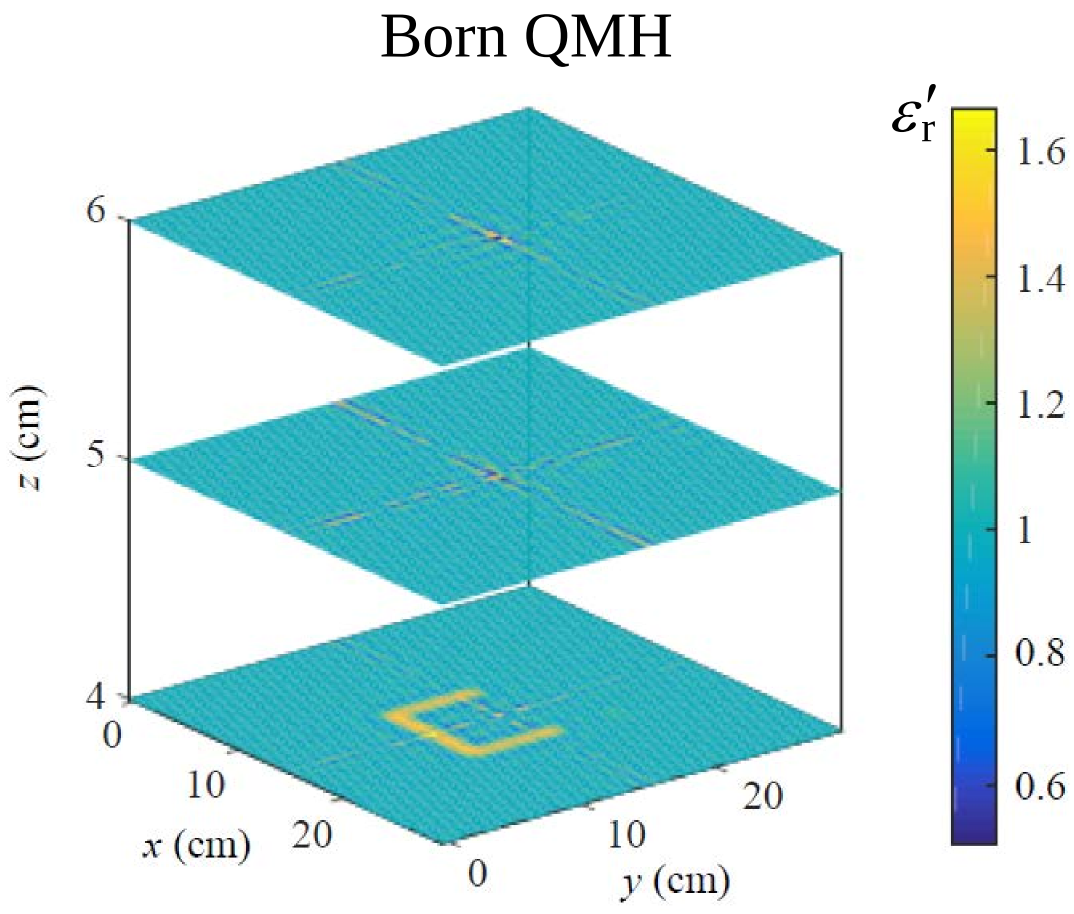

[Tajik *et al.*, *JPIER*-B 2017]

EXAMPLE: POST-INVERSION FILTERING – 2

- before IFFT, 2-D contrast solution in k-space is filtered by 4th order Butterworth filter
  - 3-dB cut-off at $\bar{K}_{\max} = 100\pi$
  - 10-dB cut-off at $1.1\bar{K}_{\max} = 110\pi$

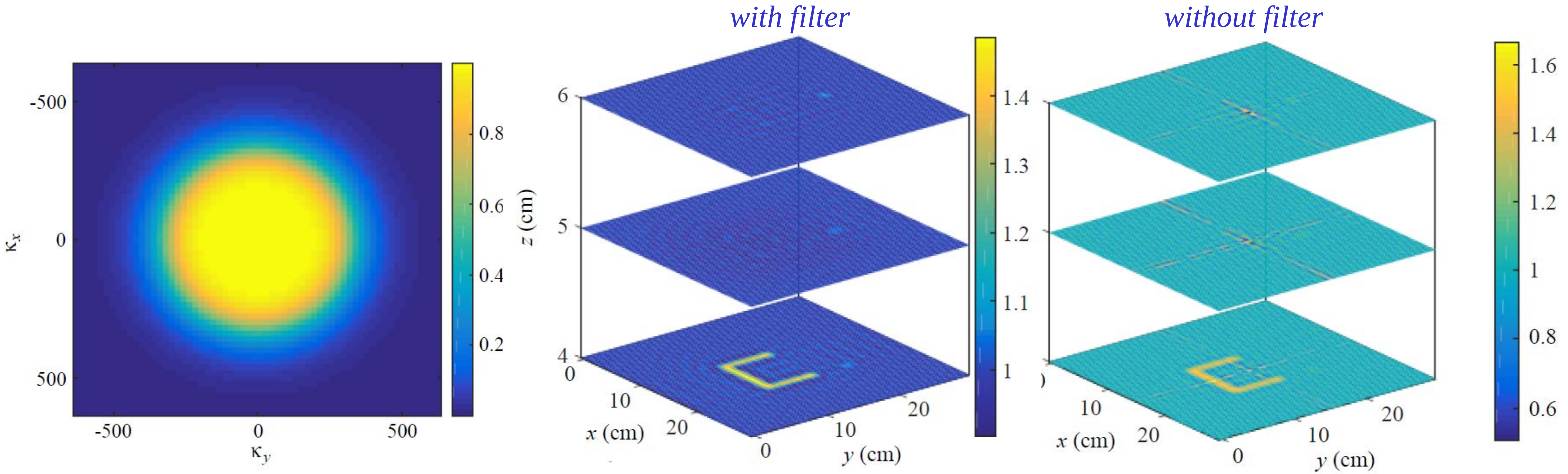

[Tajik *et al.*, *JPIER*-B 2017]

BRIEF OVERVIEW OF NONLINEAR INVERSION STRATEGIES

NONLINEAR INVERSION: SOLVING DATA AND STATE EQUATIONS

FORWARD MODELS:

$$\underbrace{F(\boldsymbol{x}) = \boldsymbol{d}}_{\text{data equation}} \quad \underbrace{\mathcal{L}_{\mathrm{ME}}\{\boldsymbol{x}, \boldsymbol{E}\} = \boldsymbol{E}}_{\text{state equations}}$$

INVERSION:

$$\underbrace{\boldsymbol{x} = F^{-1}\{\boldsymbol{d}\}}_{\substack{\text{solving}\\ \text{data equation}}} \text{ subject to } \mathcal{L}_{\mathrm{ME}}\{\boldsymbol{x}, \boldsymbol{E}\} = \boldsymbol{E}$$

data equation:

$$\underbrace{\mathbf{E}^{\mathrm{sc}}(\mathbf{r} \in S_{\mathrm{a}})}_{\text{data}} = \iiint_{V_{\mathrm{s}}} K(\mathbf{r}')\underline{\underline{\mathbf{G}}}_{\mathrm{b}}(\mathbf{r}, \mathbf{r}') \cdot \mathbf{E}(\mathbf{r}')d\mathbf{r}'$$

- the unknown is the contrast
- ensures that for a given internal field the forward model matches the data

reconstruction is an interplay of the two equations

state equation:

$$\underbrace{\mathbf{E}(\mathbf{r} \in V_{\mathrm{s}})}_{\text{internal field}} = \iiint_{V_{\mathrm{s}}} K(\mathbf{r}')\underline{\underline{\mathbf{G}}}_{\mathrm{b}}(\mathbf{r}, \mathbf{r}') \cdot \mathbf{E}(\mathbf{r}')d\mathbf{r}'$$

- the unknown is the internal field
- ensures that for a given contrast the internal field satisfies Maxwell's eqns.

NONLINEAR INVERSION: SOLVING DATA AND STATE EQUATIONS

[Nikolova, *Introduction to Microwave Imaging*, 2017]

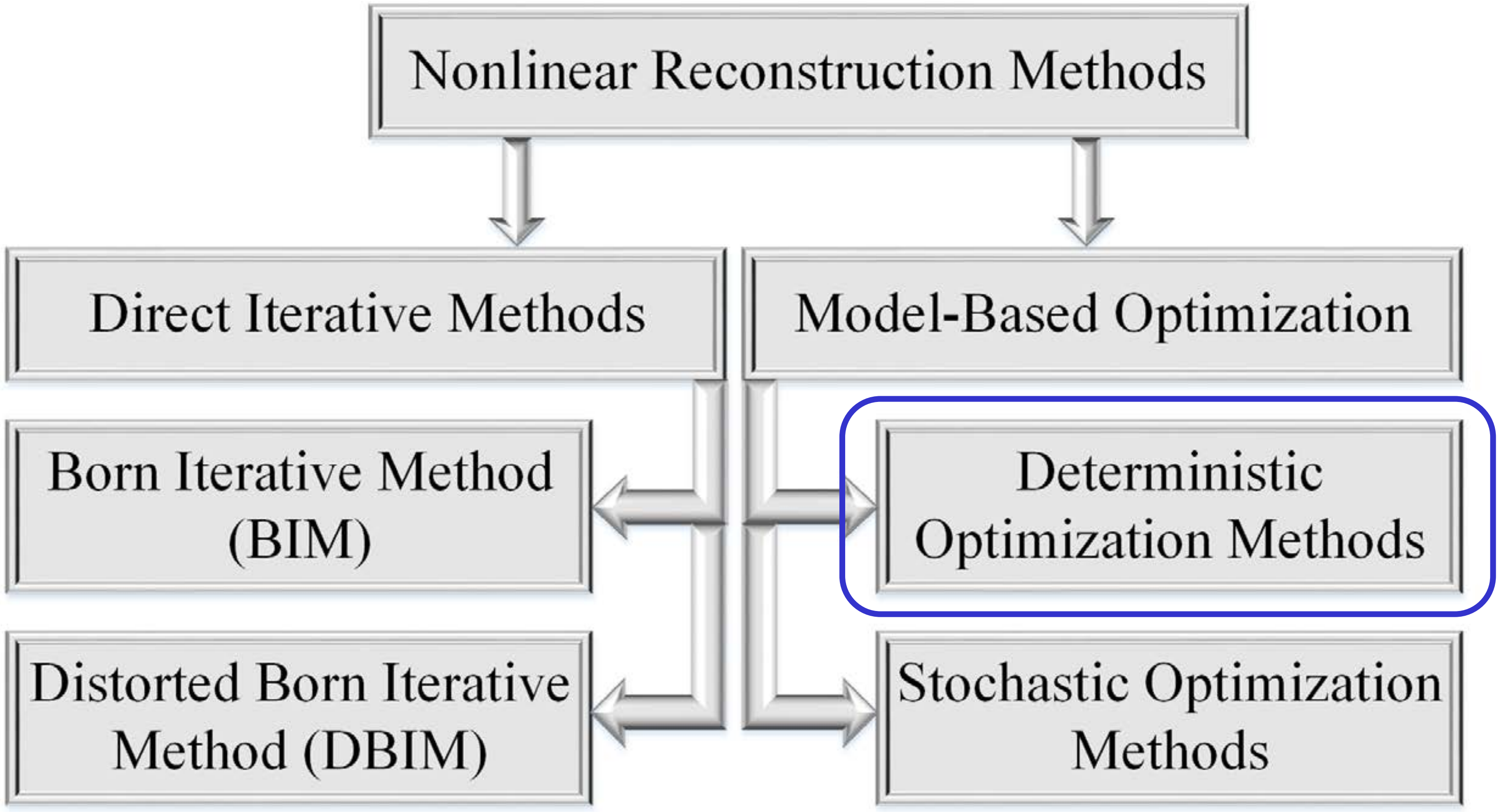

OPTIMIZATION-BASED NONLINEAR INVERSION

- formulating the objective (cost) function

$$\boldsymbol{K}^* = \arg\min_{\boldsymbol{K}} \underbrace{\left[\alpha \left\|\boldsymbol{R}_{\text{data}}\right\| + \beta \left\|\boldsymbol{R}_{\text{state}}\right\| + \gamma \left\|\boldsymbol{P}\right\|\right]}_{\text{objective function } F}$$

[Pastorino, *Microwave Imaging*, 2010]

$$\boldsymbol{R}_{\text{data}} = \bar{\boldsymbol{D}}(\bar{\mathbf{E}}^{\text{sc}}) - \boldsymbol{D}(\boldsymbol{K}, \mathbf{E}^{\text{sc}})$$ data residual (error)

$$\boldsymbol{R}_{\text{state}} = \mathbf{E}^{\text{tot}}_{\text{Tx}} - \int_{V_{\text{s}}} (K \cdot \underline{\underline{\mathbf{G}}}_{\text{b}} \cdot \mathbf{E}^{\text{tot}}_{\text{Tx}}) d\mathbf{r}'$$ state residual

$\boldsymbol{P}$ – physical constraints, *a priori* information, regularization terms

- objective function ensures the simultaneous fulfillment of the data and the state equations

NEWTON-KANTOROVICH OPTIMIZATION-BASED RECONSTRUCTION

[Roger, *IEEE Trans. Antennas Propag.* 29 (2), Mar. 1981; Joachimowicz *et al.*, *Trans. IEEE Antennas Propag.* 39 (12), 1991]

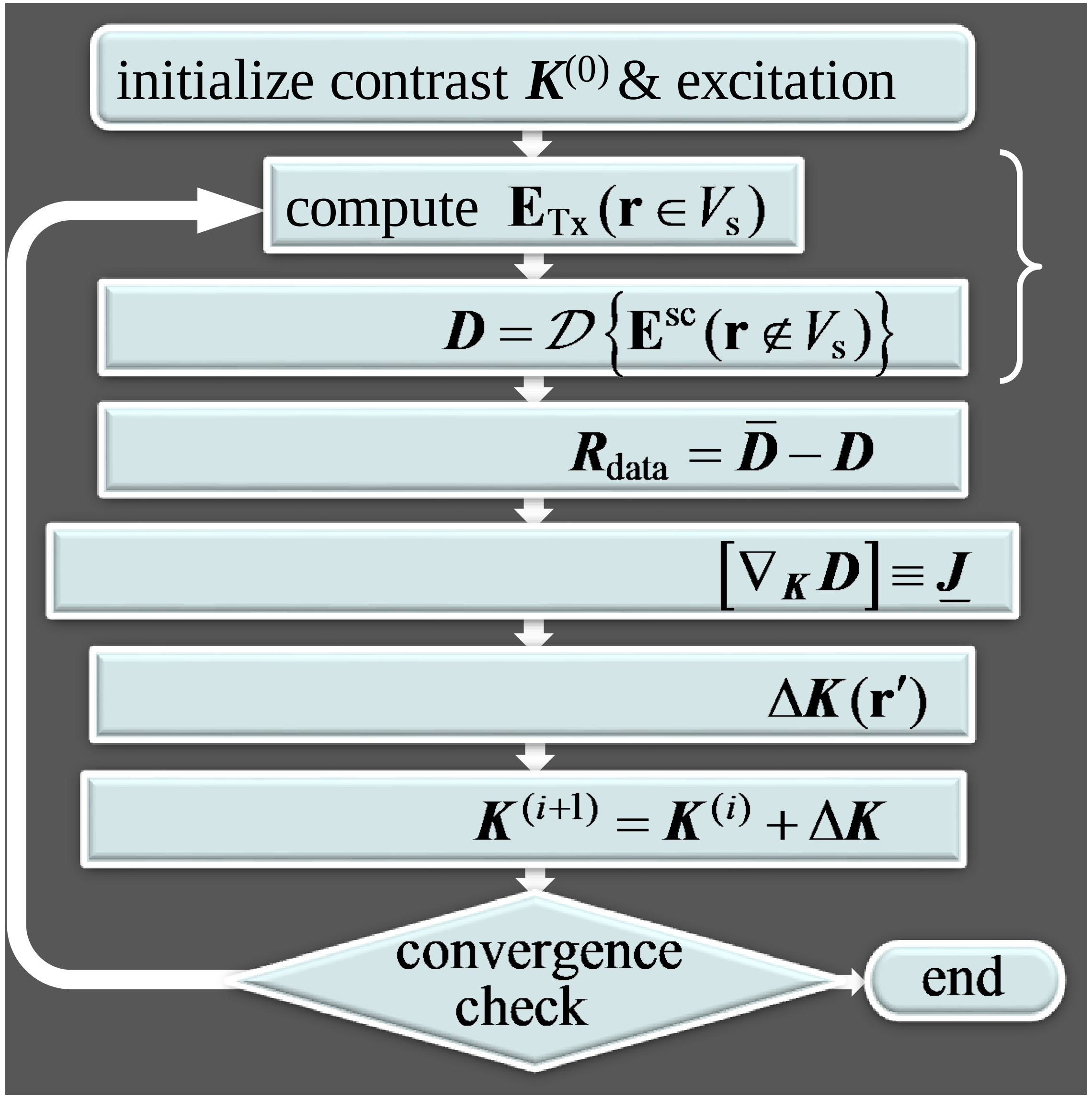

EM simulation (forward problem)

adjoint sensitivity analysis

[Section 3.2, in Nikolova, *Introduction to Microwave Imaging*, 2017]

$$\Delta \boldsymbol{K} = \left[\underline{\boldsymbol{J}}^* \underline{\boldsymbol{J}}\right]^{-1} \underline{\boldsymbol{J}}^* \boldsymbol{R}_{\mathrm{data}}$$

$$\Delta \boldsymbol{K} = \left[\underline{\boldsymbol{J}}^* \underline{\boldsymbol{J}} + \alpha \underline{\boldsymbol{I}}\right]^{-1} \underline{\boldsymbol{J}}^* \boldsymbol{R}_{\mathrm{data}}$$

objective function $F < e_F$

contrast $\|\Delta \boldsymbol{K}\| < e_K$

NONLINEAR INVERSION: SOLVING DATA AND STATE EQUATIONS

[Nikolova, *Introduction to Microwave Imaging*, 2017]

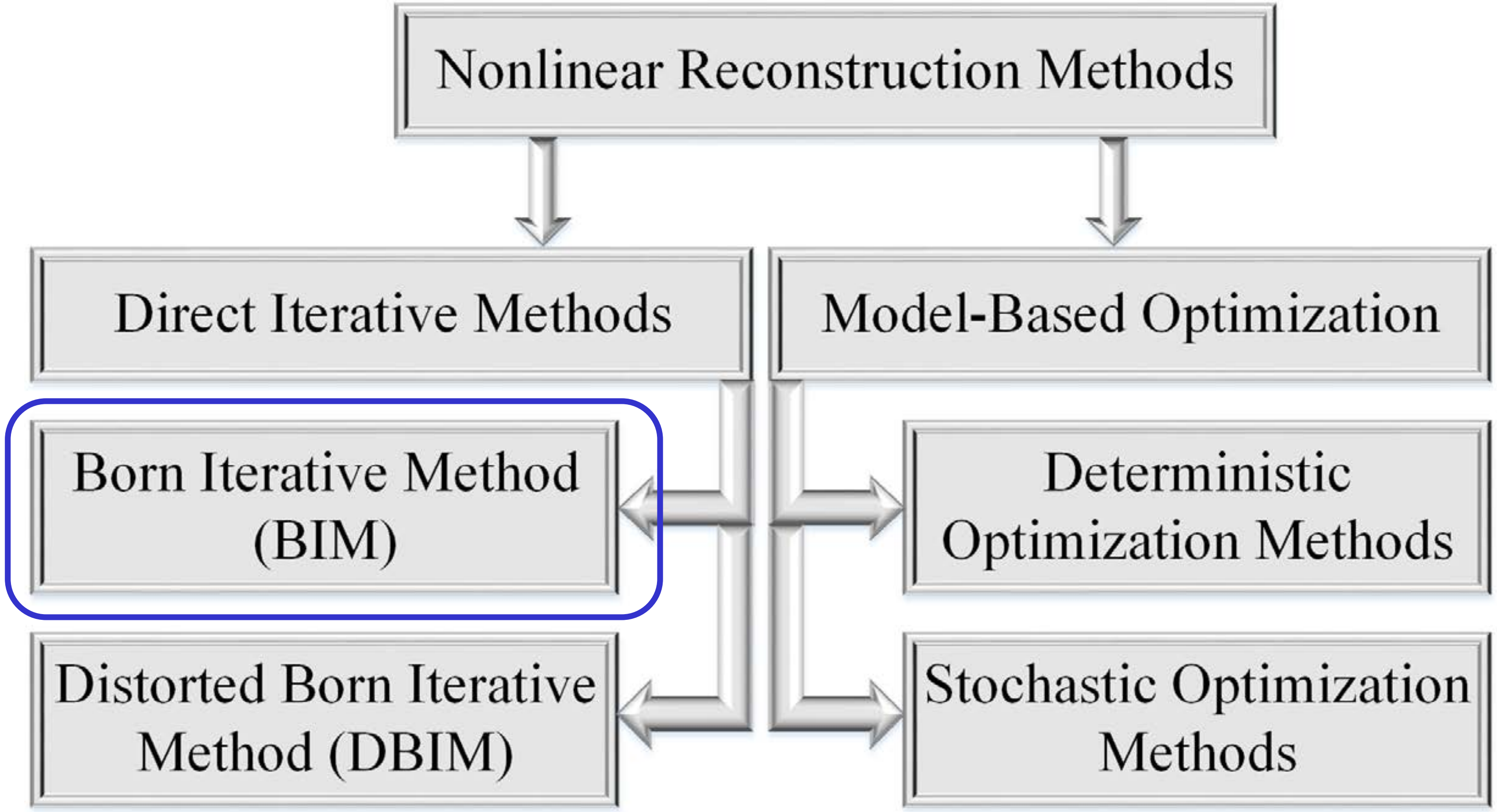

BORN ITERATIVE METHOD (BIM): FLOWCHART

[Wang&Chew, *Int. J. Imaging Systems & Tech.*, 1989]

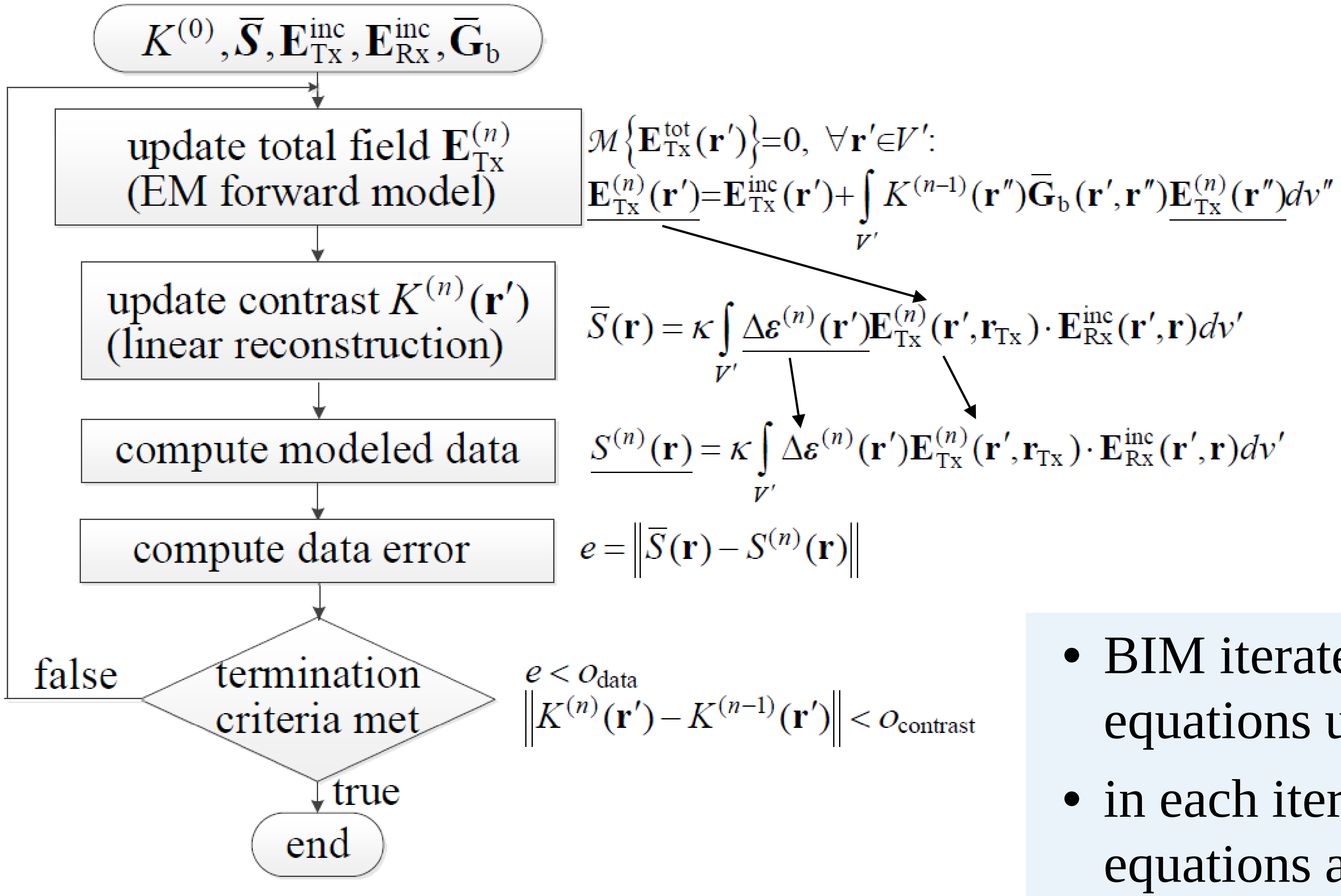

[Nikolova, *Introduction to Microwave Imaging*, 2017]

- BIM iterates between state and data equations until convergence is achieved
- in each iteration, both of these equations are linear

NONLINEAR INVERSION: SOLVING DATA AND STATE EQUATIONS

[Nikolova, *Introduction to Microwave Imaging*, 2017]

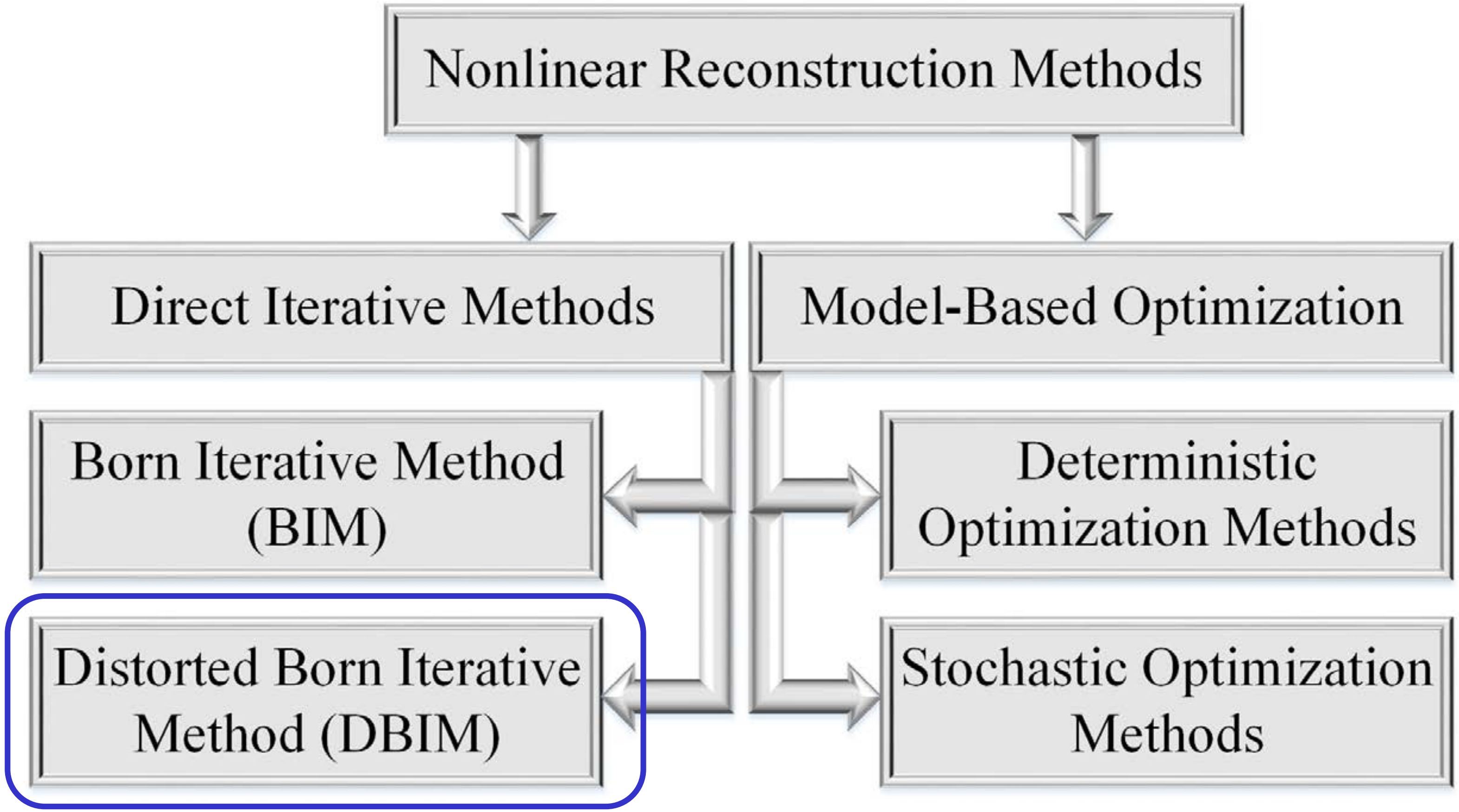

DISTORTED BORN ITERATIVE METHOD (DBIM): FLOWCHART

[Wang&Chew, *IEEE Trans. Med. Imaging*, 1990]

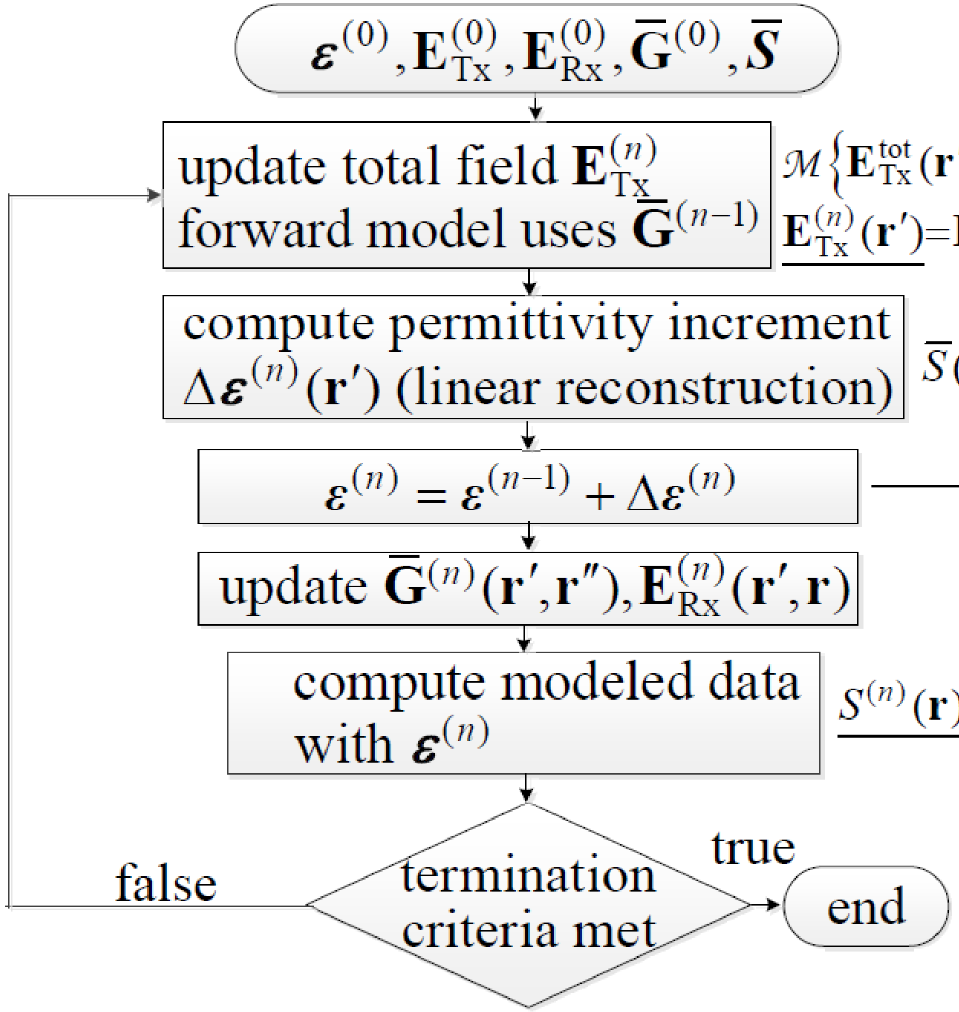

$$\mathcal{M}\left\{\mathbf{E}_{\mathrm{Tx}}^{\mathrm{tot}}(\mathbf{r}')\right\}=0,\ \forall \mathbf{r}'\in V':$$

$$\underline{\mathbf{E}_{\mathrm{Tx}}^{(n)}(\mathbf{r}')}=\mathbf{E}_{\mathrm{Tx}}^{(n-1)}(\mathbf{r}')+\int_{V'} K^{(n-1)}(\mathbf{r}'')\bar{\mathbf{G}}^{(n-1)}(\mathbf{r}',\mathbf{r}'')\underline{\mathbf{E}_{\mathrm{Tx}}^{(n-1)}(\mathbf{r}'')}dv''$$

$$\bar{S}(\mathbf{r})=\kappa\int_{V'}\underline{\Delta\varepsilon^{(n)}(\mathbf{r}')}\mathbf{E}_{\mathrm{Tx}}^{(n)}(\mathbf{r}',\mathbf{r}_{\mathrm{Tx}})\cdot\mathbf{E}_{\mathrm{Rx}}^{(n-1)}(\mathbf{r}',\mathbf{r})dv'$$

$$\underline{S^{(n)}(\mathbf{r})}=\kappa\int_{V'}\Delta\varepsilon^{(n)}(\mathbf{r}')\mathbf{E}_{\mathrm{Tx}}^{(n)}(\mathbf{r}',\mathbf{r}_{\mathrm{Tx}})\cdot\mathbf{E}_{\mathrm{Rx}}^{(n)}(\mathbf{r}',\mathbf{r})dv'$$

DBIM views the permittivity distribution in the previous iteration as a background medium for the current iteration

- DBIM is mathematically equivalent to the Newton-Kantorovich optimization scheme

[Remis&van den Berg, *Inverse Problems*, 2000]

[Nikolova, *Introduction to Microwave Imaging*, 2017]

MICROWAVE TISSUE IMAGING: OVERVIEW

first systematic studies date back to 1978

[Larsen & Jacobi eds., *Medical Applications of Microwave Imaging*, 1986]

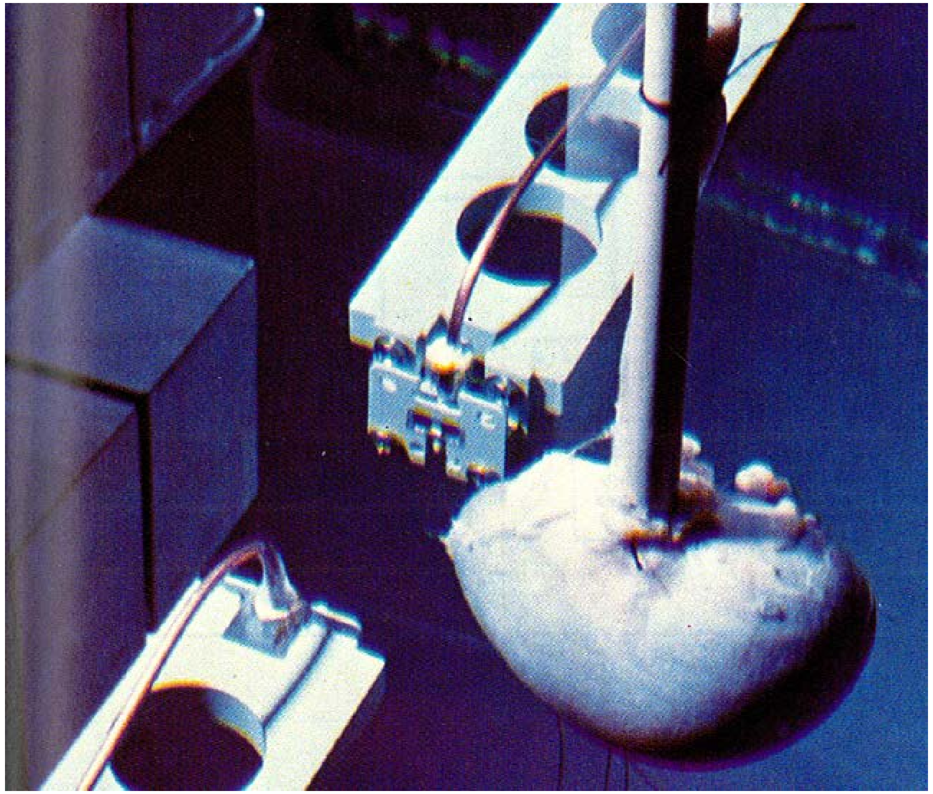

[Larsen & Jacobi, *Med. Phys*. 5 (6), 1978]

canine kidney scan in water

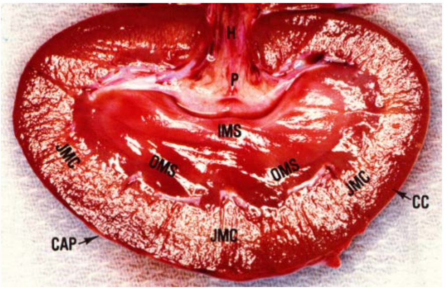

dissection

S_{21} scan, 3.9 GHz

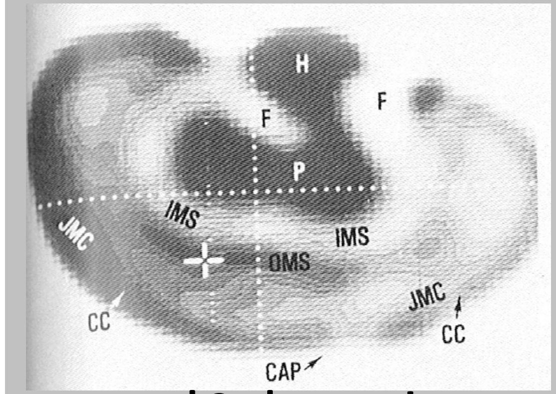

$|S_{21}|$ co-pol

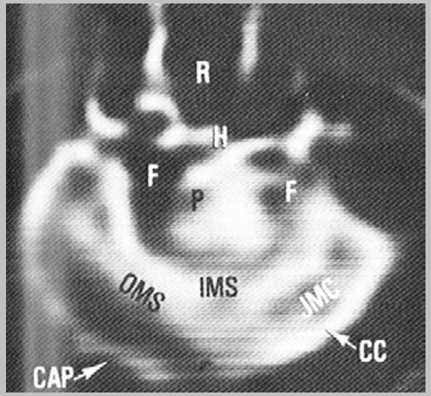

$|S_{21}|$ cross-pol

CONCLUSIONS FROM EARLY IMAGING EXPERIMENTS WITH TISSUE

- resolution on the order of a centimeter

- compromise between resolution (better at high frequencies) and penetration depth (better at low frequencies)

- optimal frequency range: 2 GHz to 8 GHz, 0.5 GHz to 3 GHz – depends on the reconstruction method

[Lin, *Proc. IEEE* 73 (2), 2005]
[Li *et al.*, *Rev. Sci. Instruments* 75 (7), 2004]
[Semenov *et al.*, *IEEE Trans. Microw. Theory Tech.* 53 (7), 2005]

- promising application in early-stage breast cancer diagnostics

  (more than 50 patents in the USA alone)

NEED FOR ALTERNATIVE MODALITIES FOR BREAST-CANCER SCREENING

[www.breastcancer.org]

- early-stage detection is crucial (size < 15 mm $\rightarrow$ survival rate $> 90\%$)

- current modalities for mass-screening are unsatisfactory

  - **mammography:** high false-negative rate esp. with radiologically dense tissue, ionizing, discomfort due to compression (mean thickness 4.4 cm to 5.4 cm)
    [Helvie *et al*., *Am. J. Roentgenol*. 163 (6), Dec. 1994]

  - **ultrasound:** operator dependent, high false-positive rate

  - **MRI:** not suitable for mass screening, requires contrast agent, somewhat high false-positive rate

ADVANTAGES AND DISADVANTAGES OF MICROWAVE IMAGING

advantages in medical diagnostics

- safe: non-ionizing radiation and low SAR (frequent check-ups)
- no need for significant compression
- cheap compact technology (deployment in GP offices)
- well suited for mass screening, prevention and early detection

disadvantages in medical diagnostics

- limited penetration (high signal loss)
- relatively low resolution

CHALLENGE #1: BREAST TISSUE HETEROGENEITY

- complex propagation environment with multiple diffraction, reflection and refraction signal paths

  - anatomical detail comparable to the radiation wavelength
  - compare with the X-ray CT propagation – a straight path!

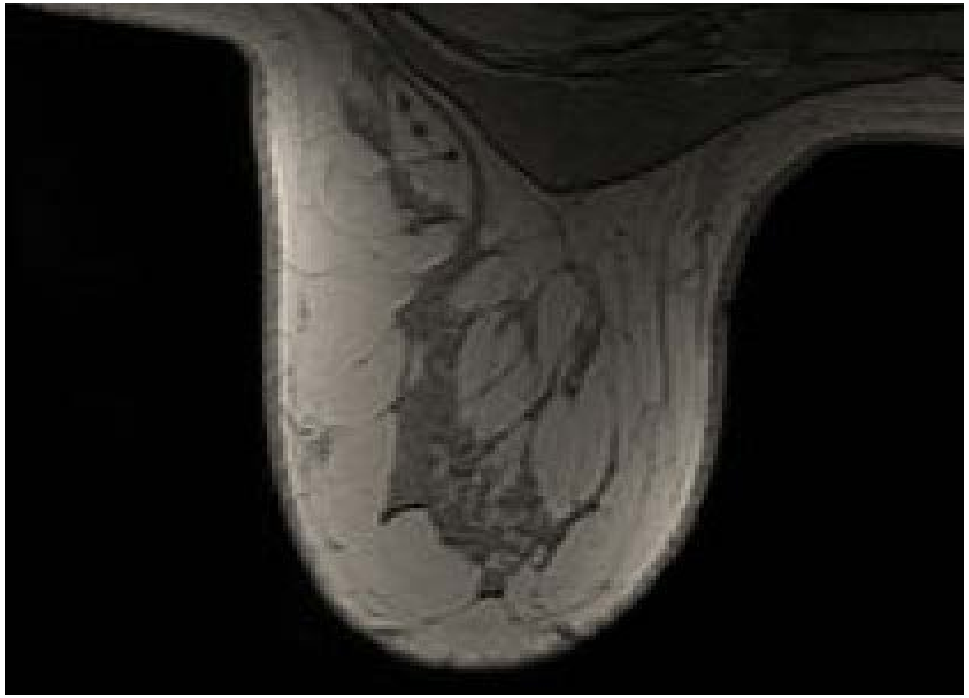

TRANSVERSE SLICE OF A T_1 WEIGHTED MR BREAST IMAGE

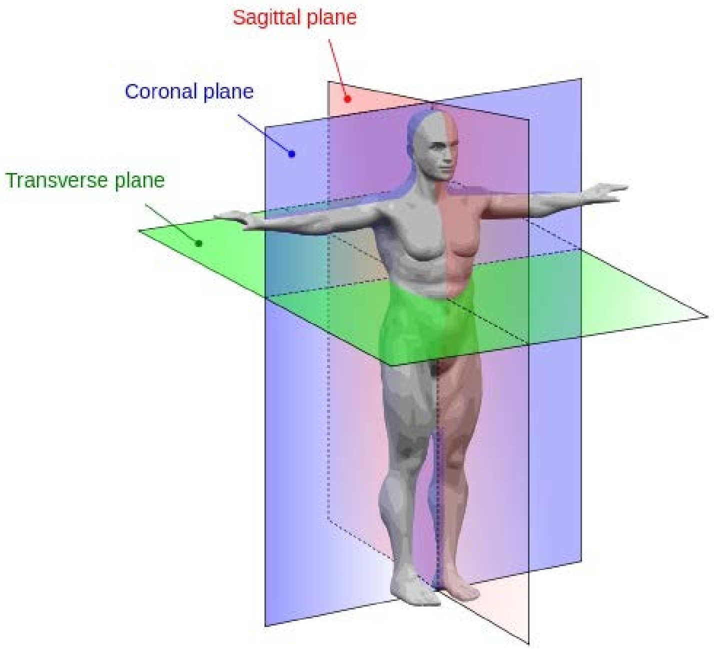

[anatomystudybuddy.wordpress.com]

CHALLENGE #2: CONTRAST IN BREAST-TISSUE CONSTITUTIVE PARAMETERS

[Sugitani *et al.*, *Applied Phys. Lett*. 104, 253702, June 2014]

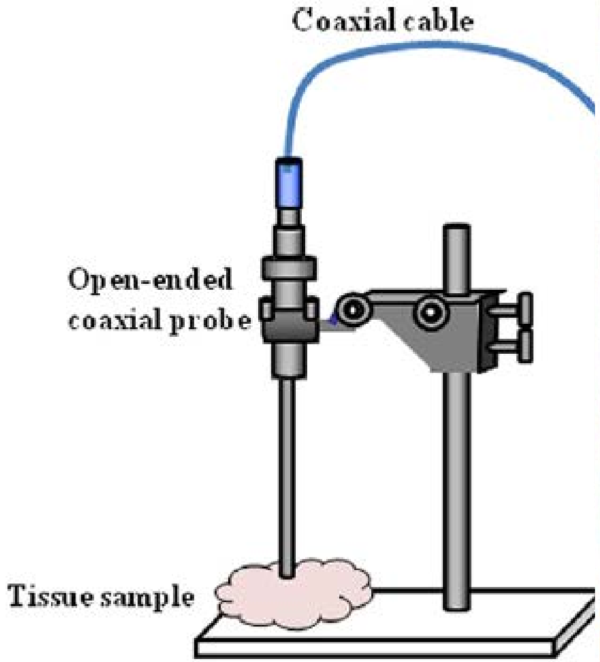

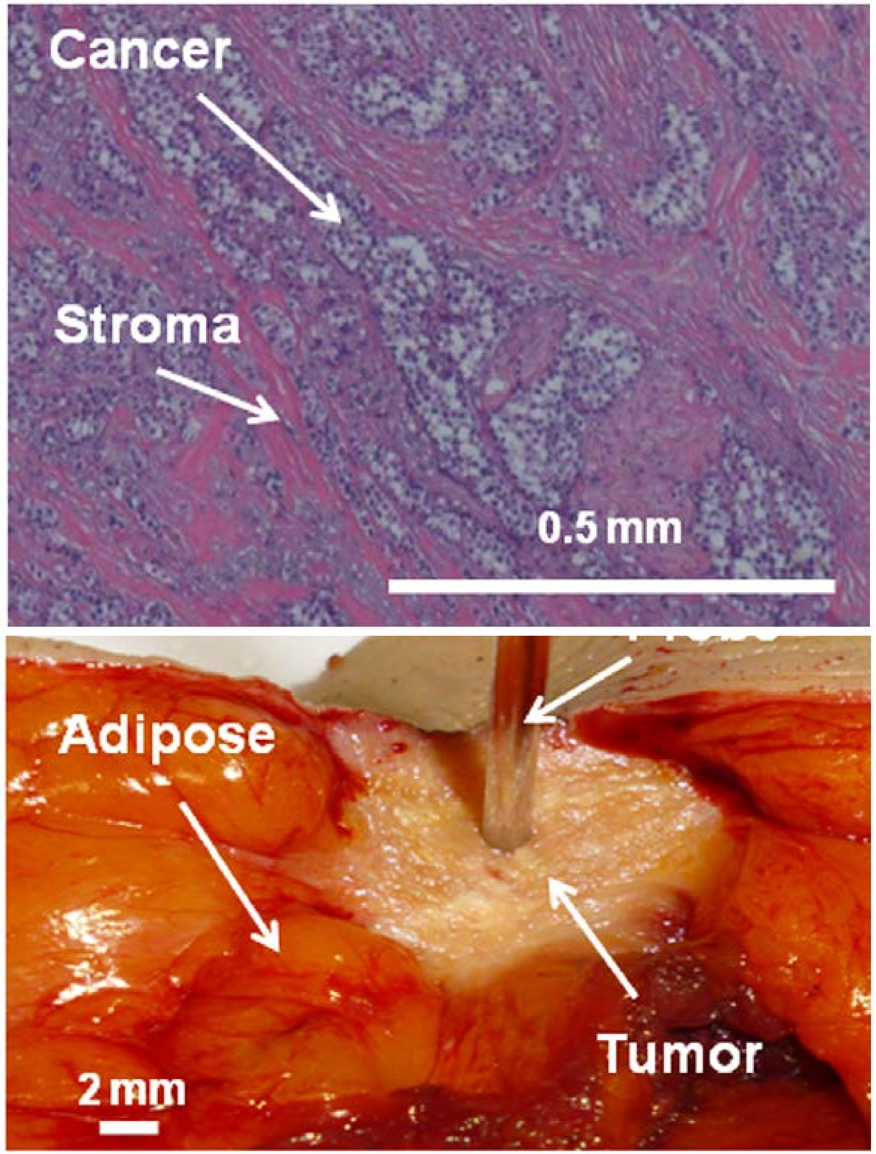

[Sugitani 2014; Figs. 1 and 2]

CHALLENGE #3: VARIABILITY IN BREAST-TISSUE DIELECTRIC PROPERTIES

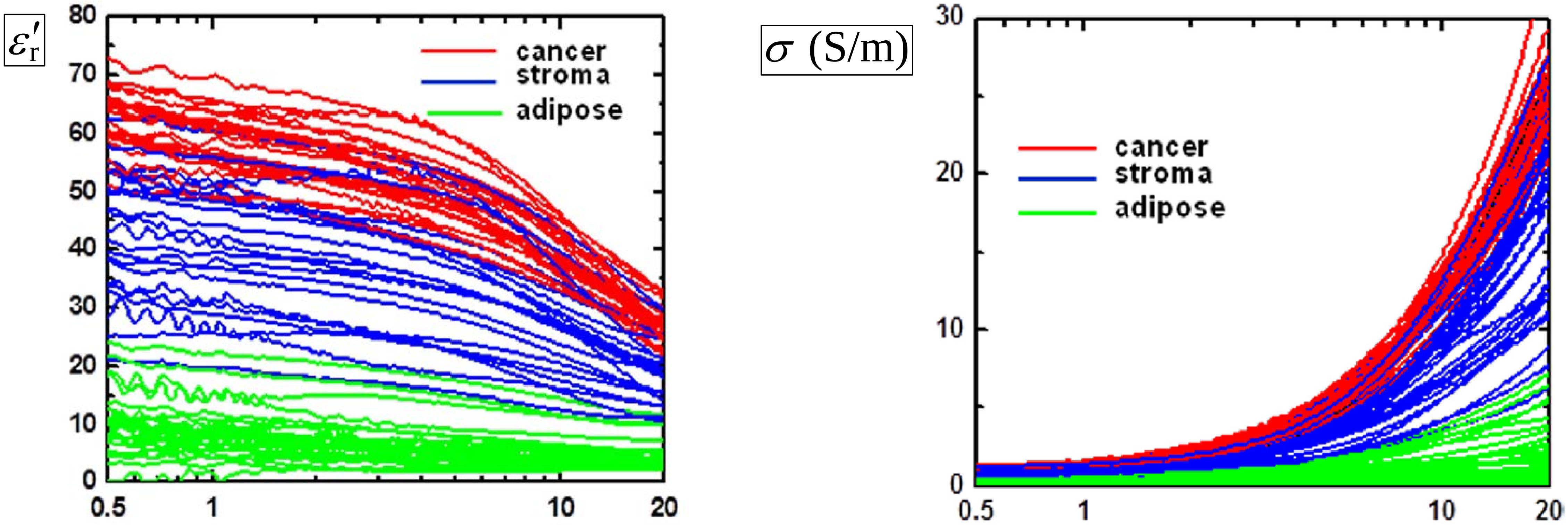

[Sugitani 2014; Fig. 3]

CHALLENGE #4: DISSIPATION IN TISSUE

Example (6 GHz, 5cm-thick tissue layer)

- muscle: $\varepsilon_r \approx 48$, $\sigma \approx 5.6$ S/m
  attenuation of about 65 Db (decrease factor > 3 million)

- stroma (fibroglandular): $\varepsilon_r \approx 50$, $\sigma \approx 5.0$ S/m
  attenuation of about 57 dB (decrease factor > half a million)

- adipose (fat): $\varepsilon_r \approx 3$, $\sigma \approx 0.3$ S/m
  attenuation of about 14 dB (decrease factor > 25)

DESIGNING THE IMAGING SYSTEM: GENERAL GUIDELINES

- prone patient positioning is common (as in MRI breast examination)
  - reduces motion artifacts due to breathing

[Mayo Foundation for Medical Education & Research]

- collect as much information as possible
  - multiple observation locations
  - illumination diversity
  - polarization diversity
  - multiple samples in UWB frequency range (or time sampling)
  - prior information about patient + continuous monitoring

DESIGNING THE IMAGING SYSTEM: ACQUISITION SURFACES

cylindrical scans – require coupling liquids

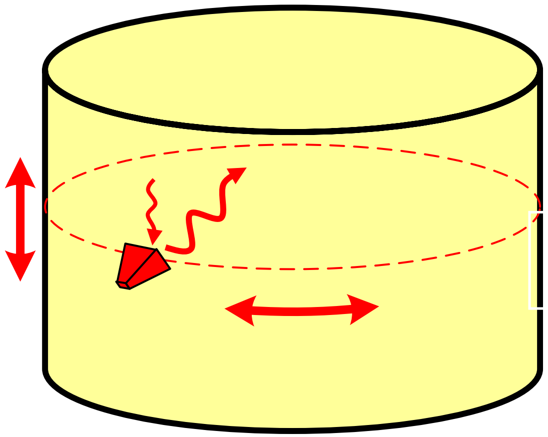

monostatic

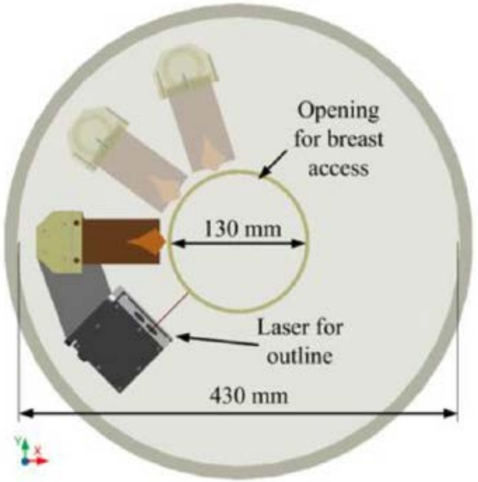

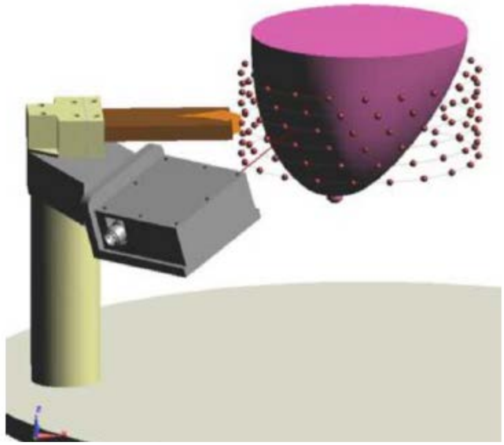

[Fear *et al.*, *IEEE Trans. Microw. Theory Tech.* 61 (5), 2013]

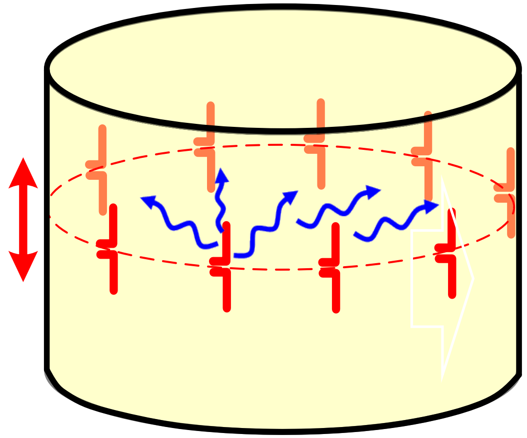

multistatic

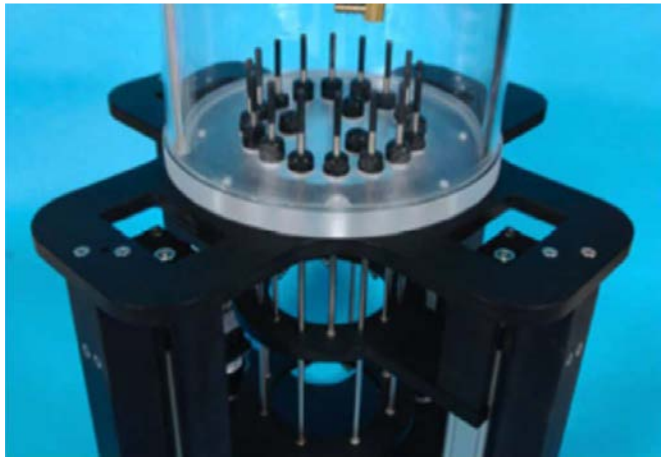

[Grzegorczyk *et al.*, *IEEE Trans. Med. Imaging* 31 (8), 2012]

<u>hemispherical scans</u> – use coupling gels

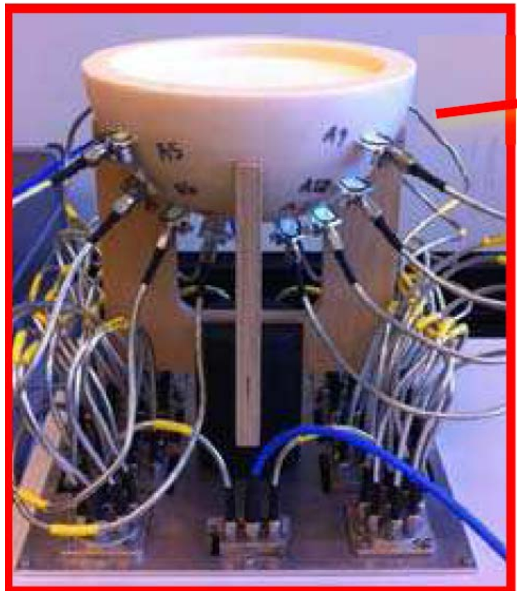

[Porter *et al.*, *IEEE Antennas Wirel. Propag. Lett.* 12, 2013]

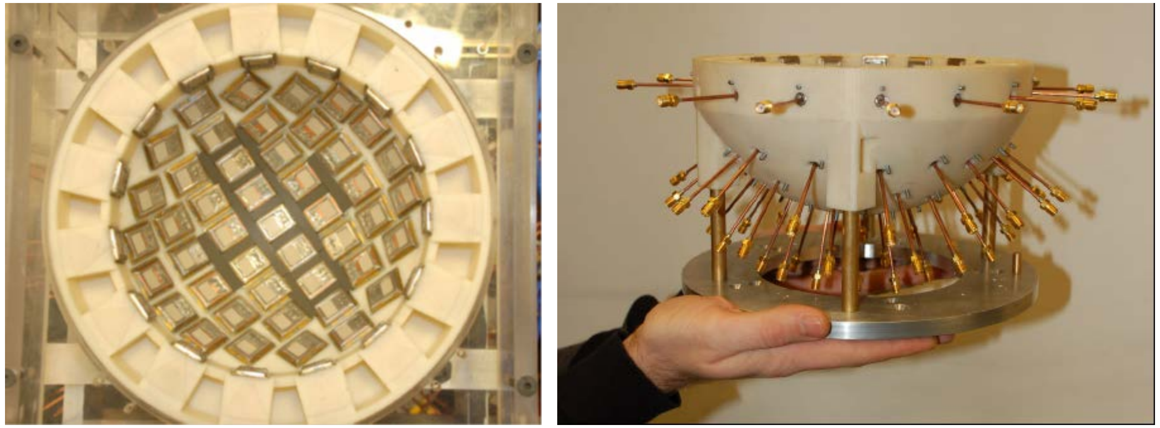

[Klemm *et al.*, *EuCAP 2011*, Apr. 2011]

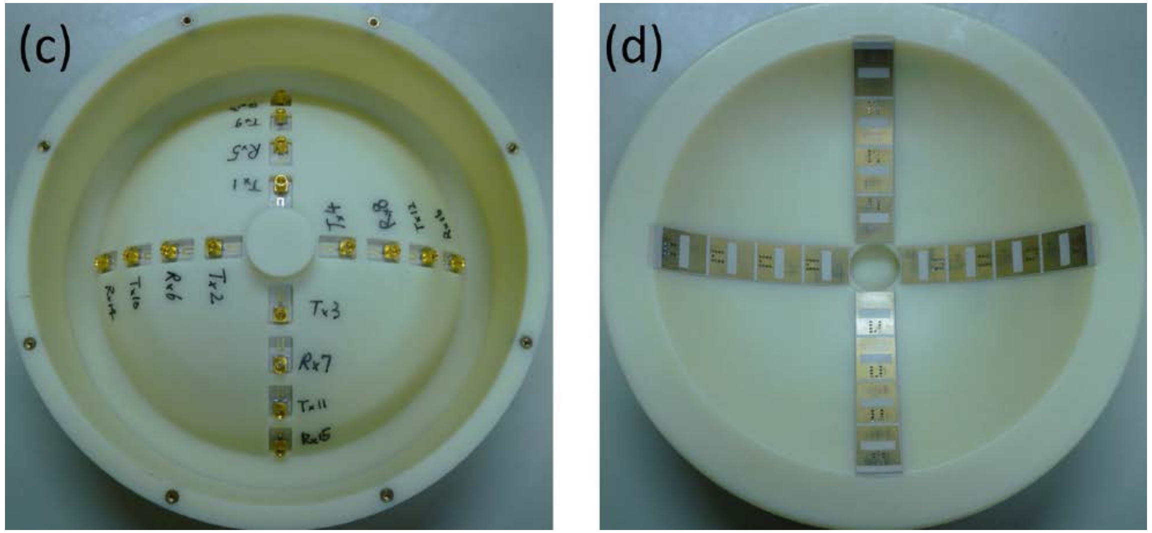

[Song *et al.*, *Nature Scientific Rep.*, Nov. 2017]

DESIGNING THE IMAGING SYSTEM: ACQUISITION SURFACES, CONT.

planar

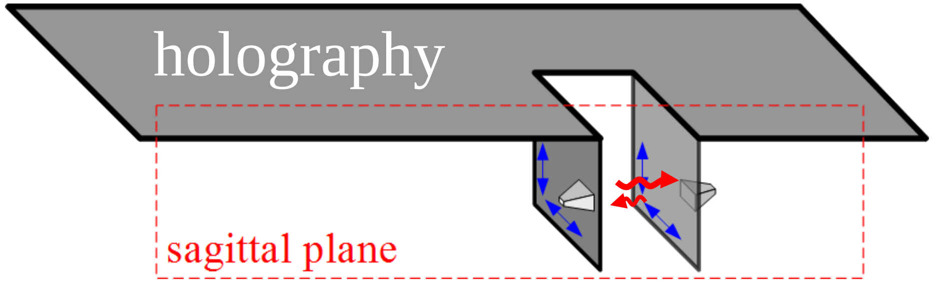

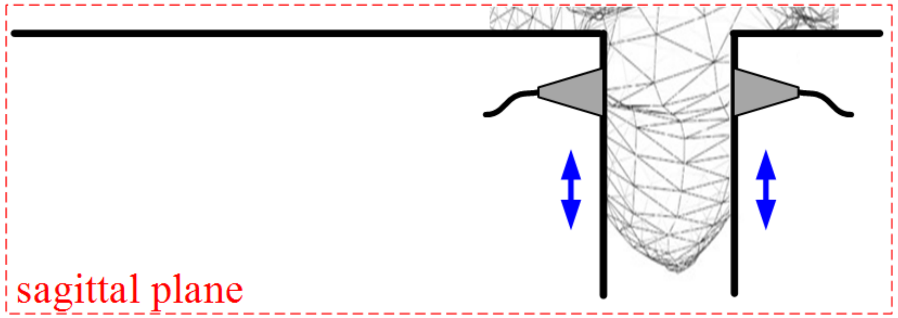

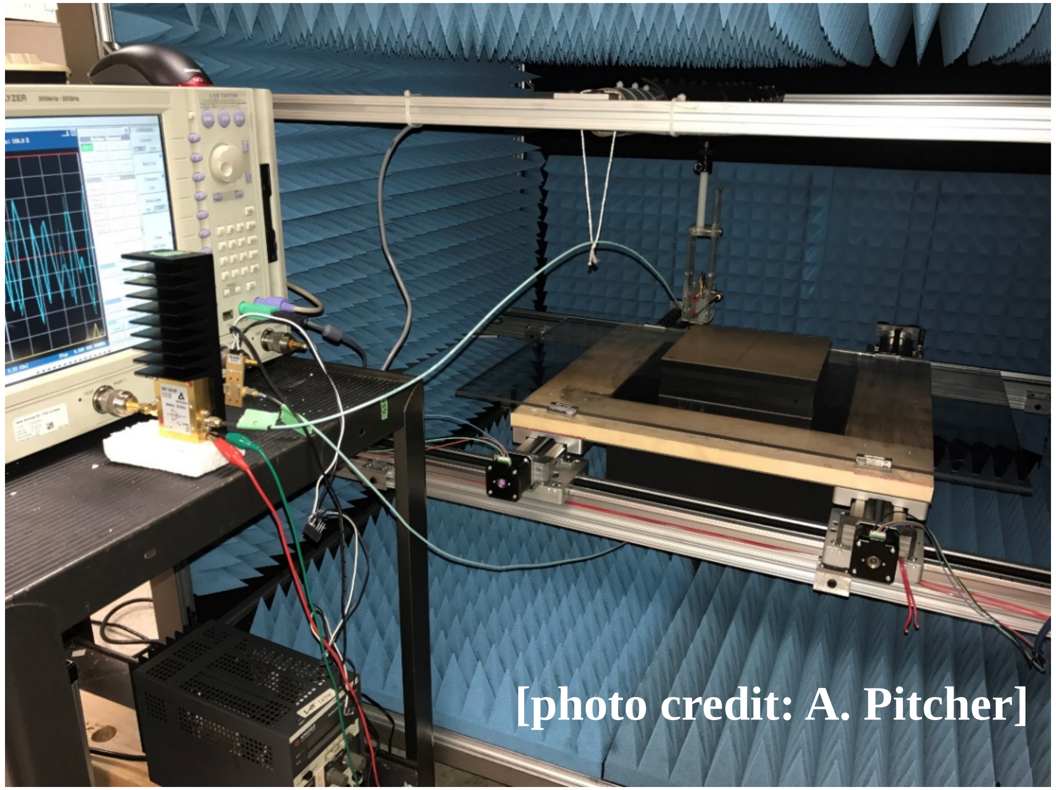

EMVi experimental lab: planar scanner

SOME PROMISING CLINICAL TRIALS: BRISTOL UNIVERSITY

[Klemm *et al.*, *IEEE Trans. Antennas Propag*. 58 (7), 2010]

- real-time reconstruction based on synthetic focusing (DAS)
- fixed multistatic 60-element hemispherical array

Klemm 2010, Figs. 5 and 7

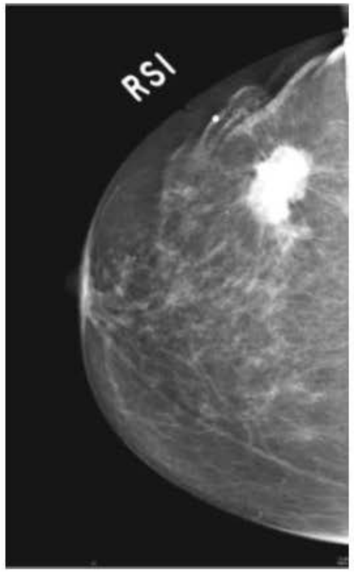

transverse X-ray

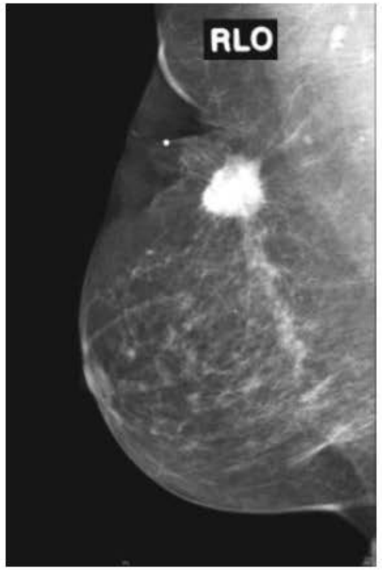

sagittal X-ray

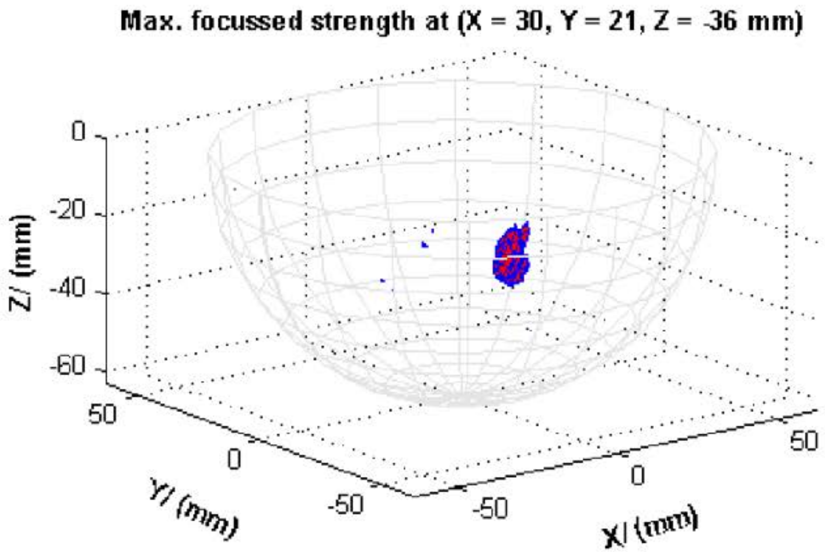

3-D radar

- radiologically translucent case with 30-mm tumor

SOME PROMISING CLINICAL TRIALS: HIROSHIMA UNIVERSITY

[Song *et al.*, *Nature Scientific Rep.*, Nov. 2017]

- real-time reconstruction based on synthetic focusing (DAS)
- handheld rotating 16-element hemispherical array

Song 2017, Fig. 7

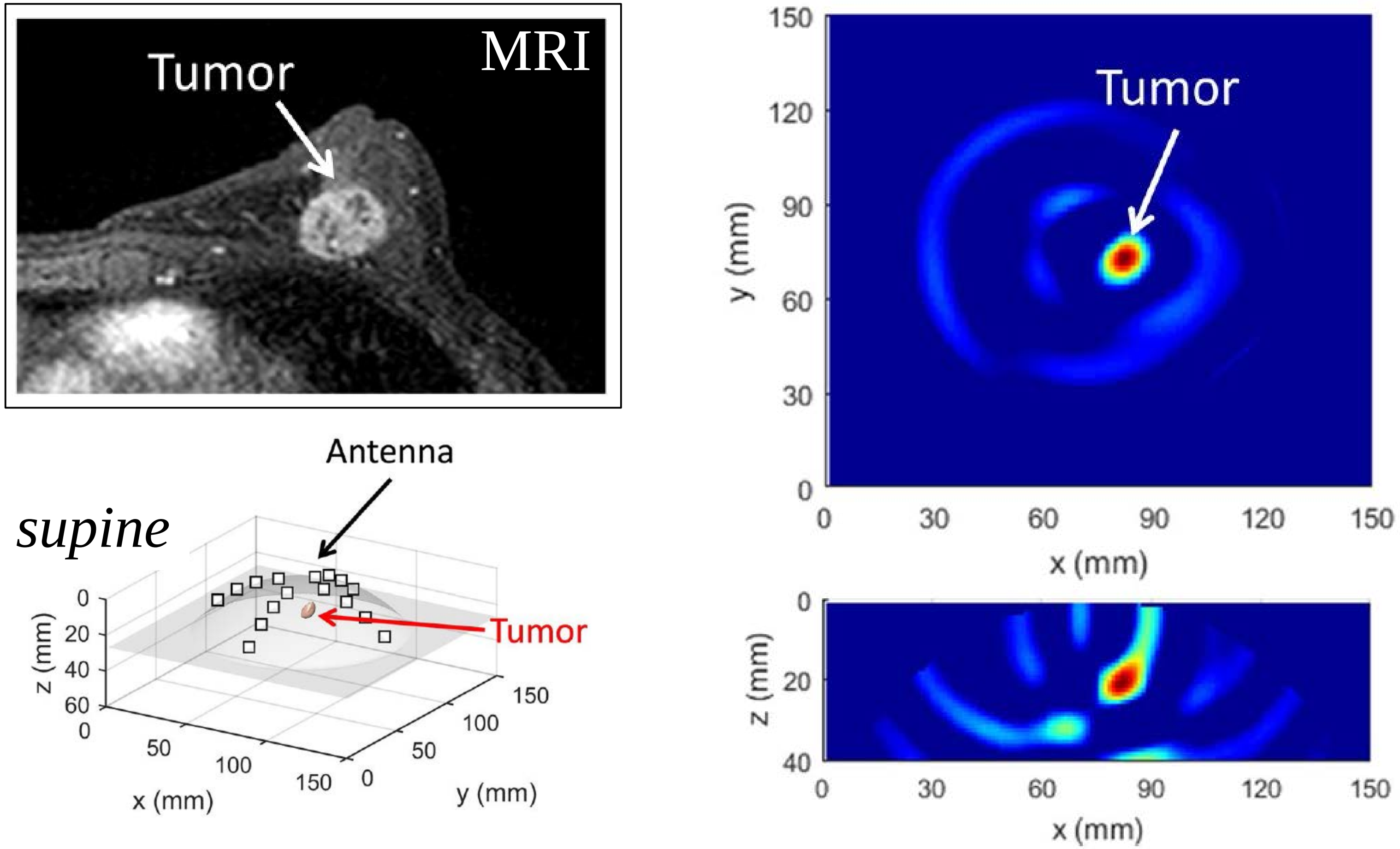

SOME PROMISING CLINICAL TRIALS: DARTMOUTH COLLEGE

[Poplack *et al.*, *Radiology* 243 (2), May 2007]

- imaging through EM-based optimization
- cylindrical tomography system
- reconstruction time: within 10 minutes

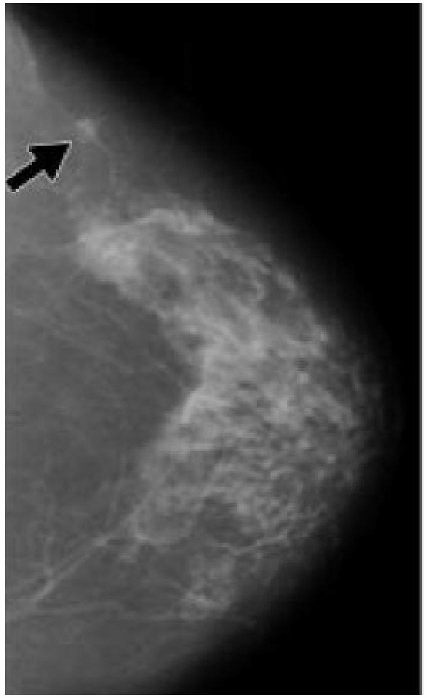

X-ray

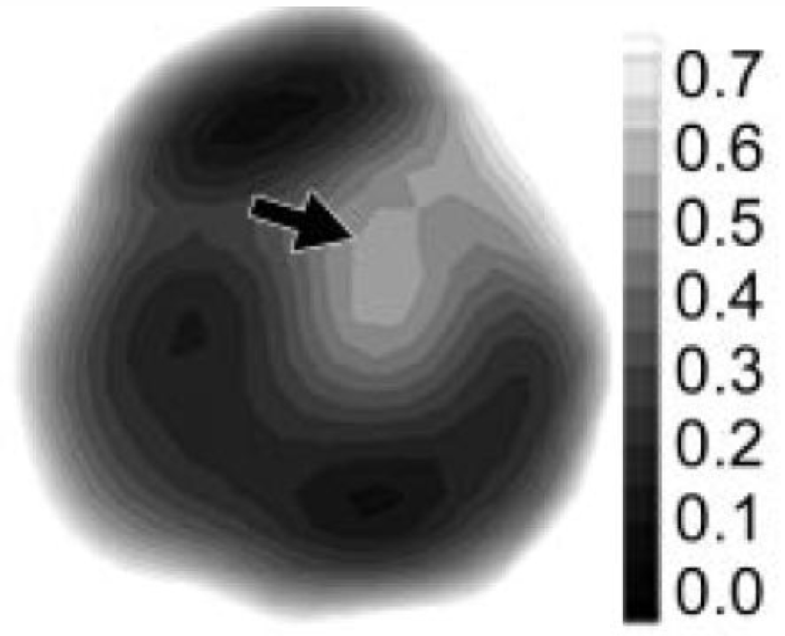

MW tomography
coronal slice

Poplack 2007, Fig. 1

MCMASTER U: OUR PRELIMINARY TESTS WITH TISSUE PHANTOMS

[Tajik *et al.*, *PIER-B*, 2017]

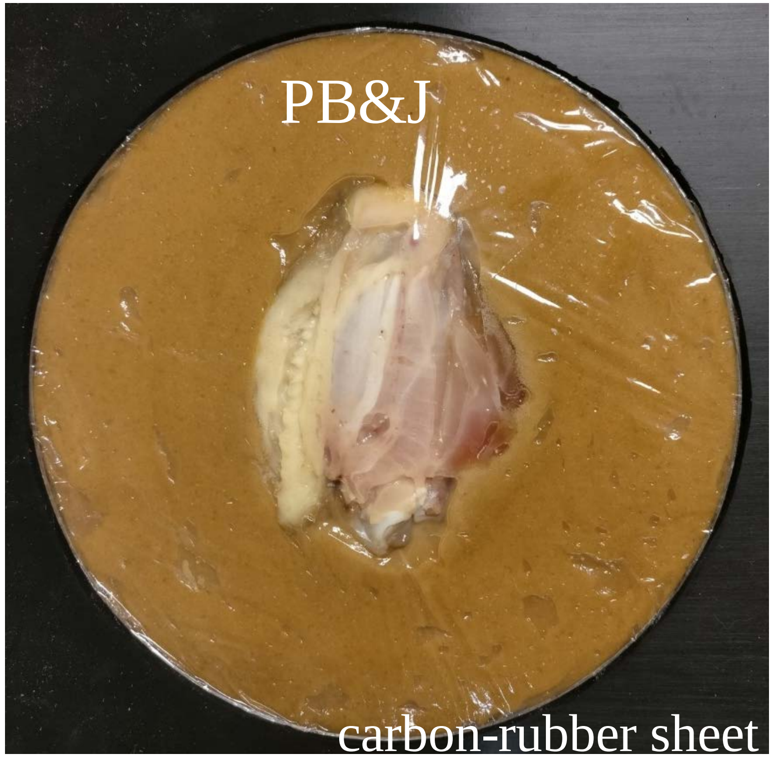

Tajik 2017, Fig. 9

Quantitative Microwave Holography (QMH) inversion (Born) <u>with apodization and *k*-space filtering</u>

- frequency sweep: from 3 GHz to 9 GHz, 61 samples
- spatial sampling step: 2 mm
- reconstruction time: < 10 s

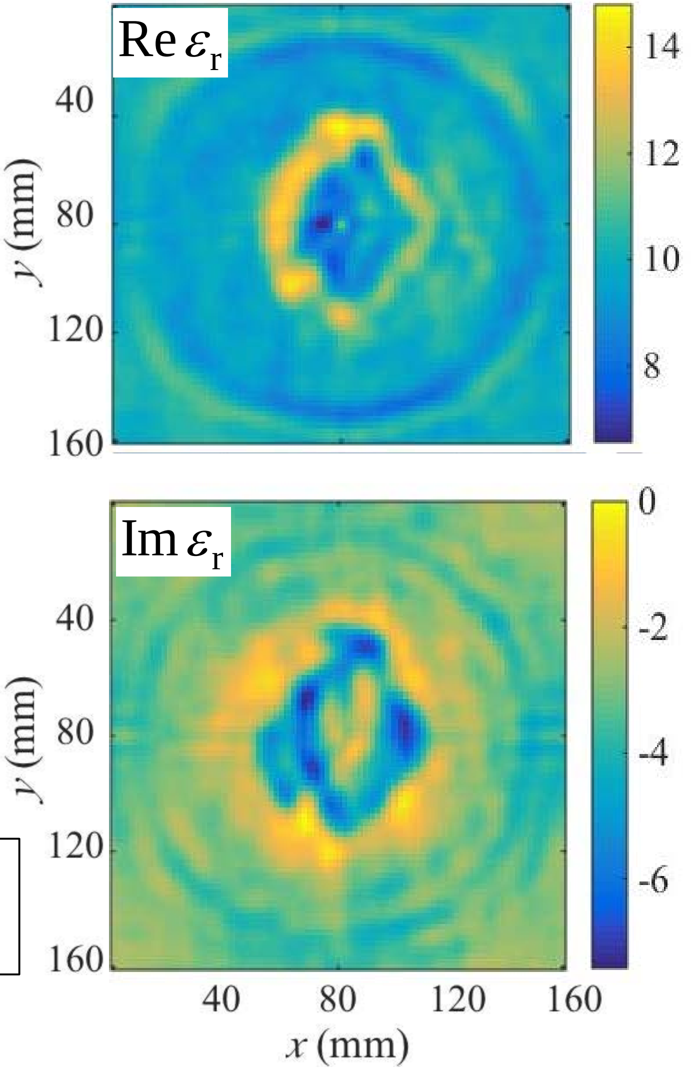

Tajik 2017, Fig. 16

MCMASTER U: TISSUE PHANTOM MEASUREMENT

[Tajik *et al.*, EuCAP 2019]

- phantom: five 1.1 cm thick carbon-rubber sheets stacked
- permittivity of carbon-rubber sheets approximates averaged *Type-2 breast tissue* (25% - 50% fibroglandular tissue, remaing fatty tissue)
- filled with fibroglandular/tumour simulants
- simulants surrounded with matched medium

Tissue	Color	Permittivity (5 GHz)
Tumour Simulant	**Blue Circles**	50 — 25i
Fibroglandular Simulant	**White**	13 — 6i
Averaged Type-2 Breast Tissue	**Brown**	7 — 3i
Absorbing Foam	**Black**	10 — 3i

- QMH (Born)
- apodization applied
- *k*-space filtering applied
- CNR data filtering applied

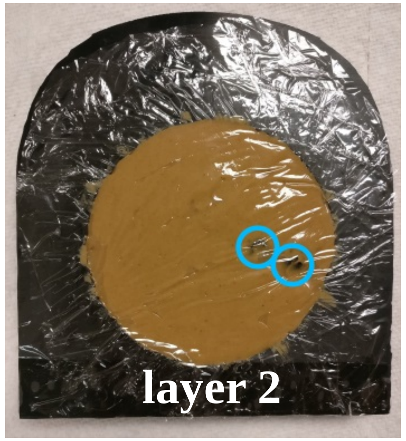

Image Credit: Daniel Tajik

MCMASTER U: TISSUE PHANTOM MEASUREMENT

[Tajik *et al.*, EuCAP 2019]

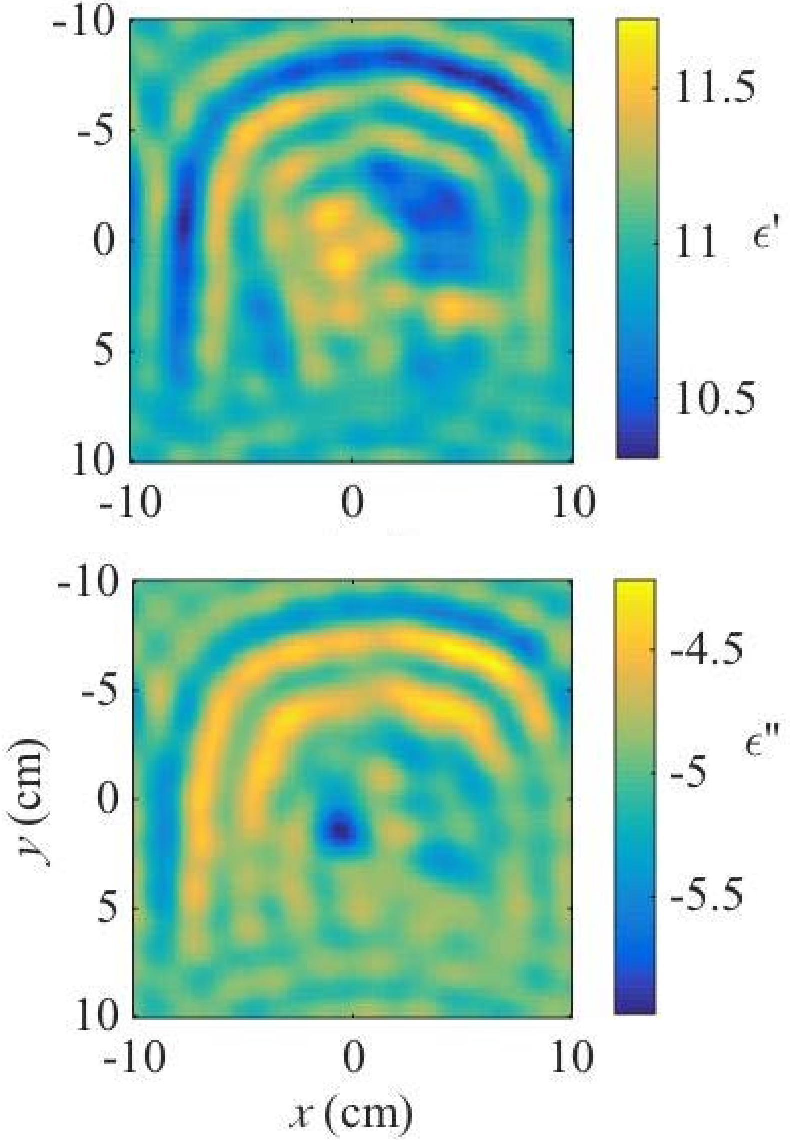

Image Credit:
Daniel Tajik

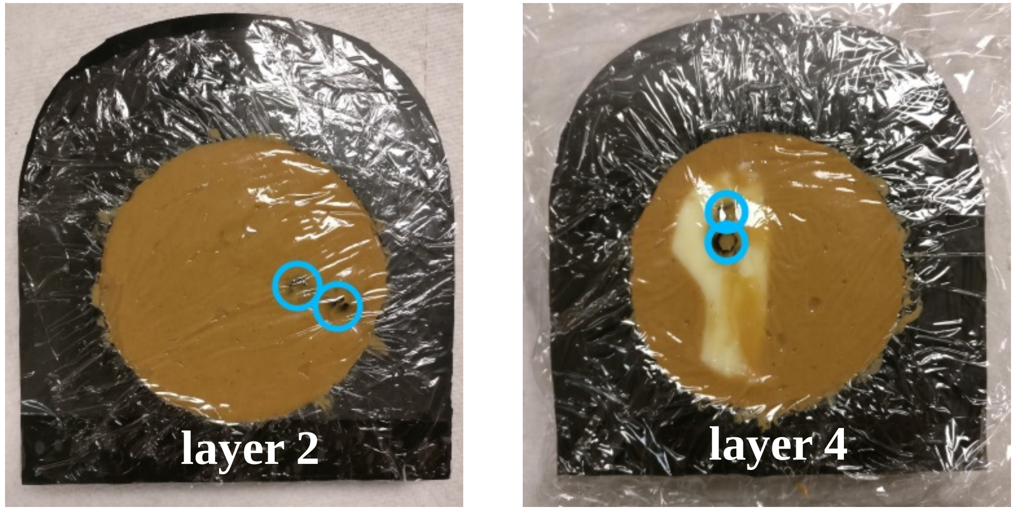

2-D images (as in mammography):
layer 2 and layer 4 are superimposed

TISSUE PHANTOM MEASUREMENT: COMPARISON WITH CT IMAGES

[Tajik *et al.*, EuCAP 2019]

Born-based QMH – 2D

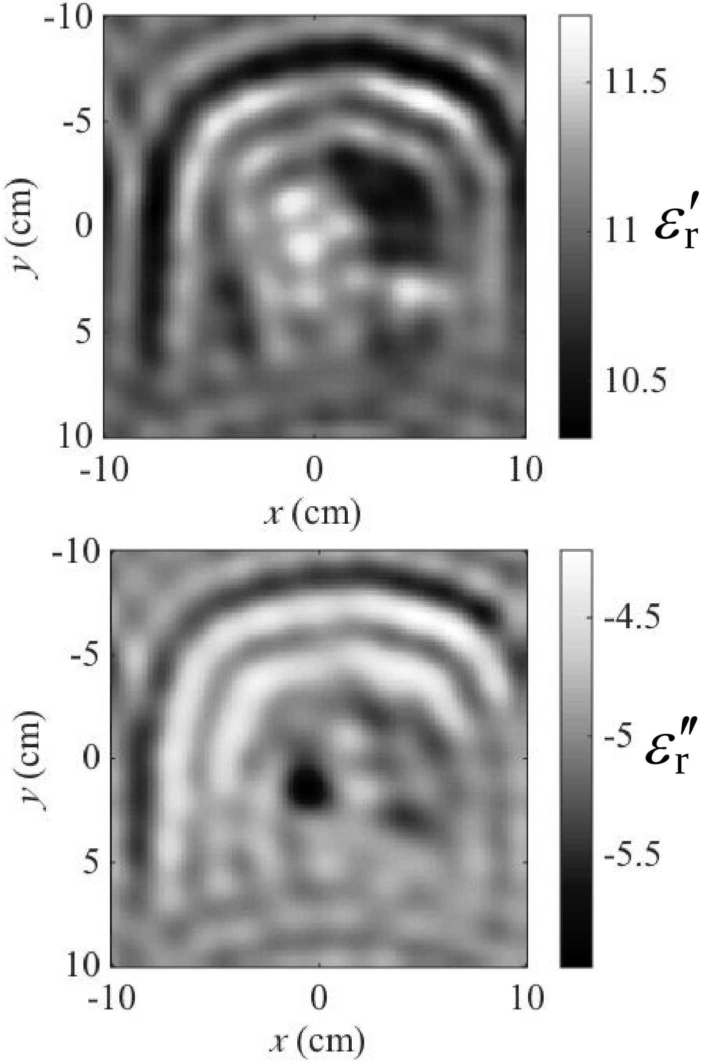

Image Credit: Daniel Tajik

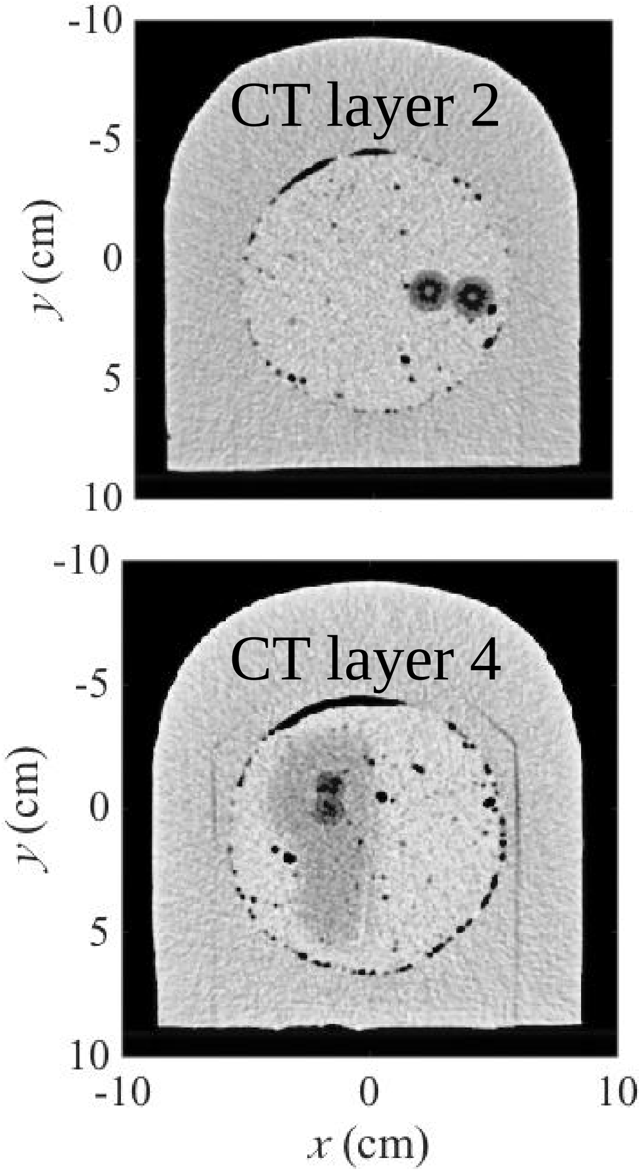

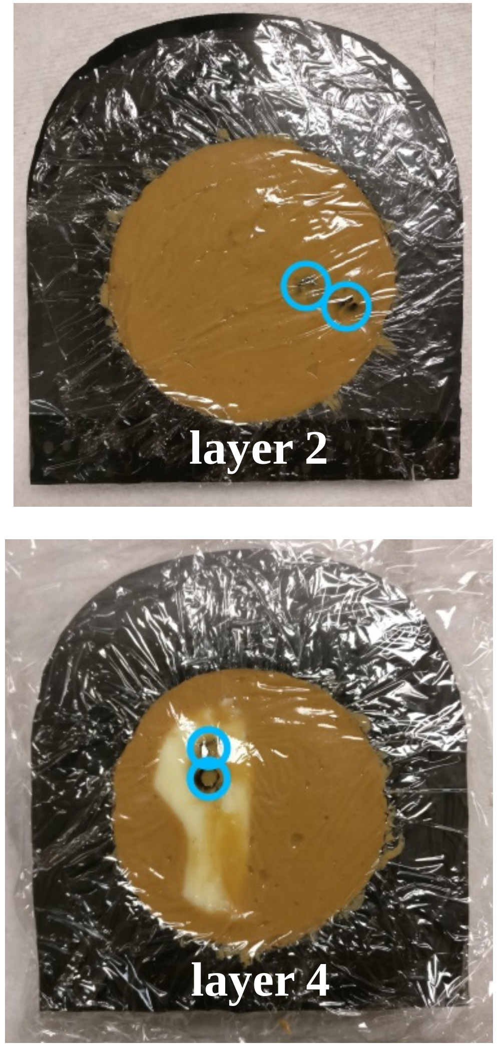

MICROWAVE TISSUE IMAGING: LOOKING FORWARD

software

- conceptually new iterative reconstruction algorithms – real-time!
- noise suppression and filtering
- system calibration and error deembedding

hardware

- toward bias-switched arrays of on-chip radios
- SDRs: improving SNR through signal encoding (e.g., OFDM radar)
  [Wiesbeck, "System concepts for the radar of the future," *EuCAP 2017* Short Course "Radar 2020"]
- contrast agents for microwave imaging (carbon and magnetic nanoparticles)

SUMMARY OF DAY THREE

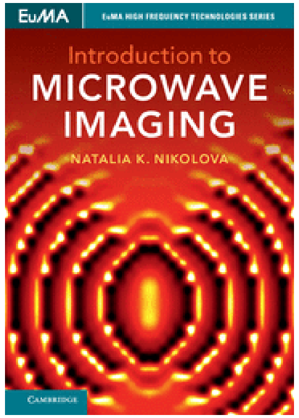

- imaging methods are subject to ***fundamental resolution limits***, which depend on the wavelength, the target viewing angle and the presence/absence of near-field scattering data
- ***inversion in k-space*** must be done with the properties of FFT in mind – ***apodization and post-inversion filtering*** are almost always beneficial
- ***noise and uncertainties*** are unavoidable in experiments – the CNR metric is critical in assessing: (i) the readiness of the acquisition system, (ii) the quality of a data set before submitting it to a reconstruction algorithm
- ***nonlinear inversion algorithms*** ensure that both the data and the state equations are satisfied (potential for better accuracy over quantitative linear reconstruction); disadvantage – use of EM simulations (increased inversion time)
- the ***advent of microwave imaging into medical diagnostics*** is promising, especially in cancer diagnostics (except for deep-body tumours)

[worldartsme.com]

THANK YOU!